On the Characteristics and Circulation of the Southwestern Atlantic Ocean

JOSEPH L. REID

Scripps Institution of Oceanography, La Jolla, Calif. 92093

WORTH D. NOWLIN, JR.

Department of Oceanography, Texas A & M University, College Station, 77843

WILLIAM C. PATZERT

Scripps Institution of Oceanography, La Jolla, Calif. 92093

(Manuscript received 3 May 1976, in revised form 2 September 1976)

ABSTRACT

The waters found within the southwestern Atlantic Ocean extend into it as separate lavers with markedly different characteristics. Along the western boundary the deeper waters, derived from the North Atlantic, are warm, highly saline, oxygen-rich and nutrient-poor. This North Atlantic Deep Water (NADW) lies within the density range of the Circumpolar Water (CPW) from the south, which is cooler, lower in salinity, very low in oxygen and very high in nutrients. Where the NADW and CPW meet in the southwestern Atlantic, the NADW separates the CPW into two layers above and below the NADW—each less saline, richer in nutrients and lower in oxygen than the NADW.

Above the upper branch of the CPW lies the Subantarctic Intermediate Water, which is lowest in salinity of all the layers. Beneath the lower branch of the CPW lies an abyssal layer derived from the mid-depths of the Weddell Sea. It is colder, less saline, lower in nutrients and higher in oxygen than the Circumpolar Water.

These layers appear to be separated vertically by density gradients which tend to be sharper at the interface than in the layers themselves. These maxima in stability, which result from the interleaving of water masses from different sources, extend over hundreds of kilometers: apparently vertical exchange processes are not strong enough to dissipate them.

Within the Argentine Basin the circulation of all except the abyssal layer appears to be anticyclonic and so tightly compressed against the western boundary that equatorward flow is observed just offshore of the poleward flow at the boundary. Waters from the north (within the Brazil current near the surface and from the North Atlantic at greater depths) flow southward along the western boundary and turn eastward near 40°S, part returning around the anticyclonic gyre and part joining the Antarctic Circumpolar Current. Likewise the Circumpolar Waters, which have entered from the Pacific, flow northward along the western boundary to about 40°S and then turn eastward, both above and below the NADW. The abyssal waters are derived from the Weddell Sea. Within the Argentine Basin they flow northward along the western boundary and turn eastward south of the Rio Grande Rise, and then southward on the western flank of the Mid-Atlantic Ridge; the abyssal flow is cyclonic beneath the anticyclonic upper circulation.

1. Introduction

The purpose of Leg 6 of the Cato expedition, carried out aboard the RV *Melville* from 5 November to 17 December 1972, was to measure the characteristics of the waters between the Mid-Atlantic Ridge and the South American coast in the vicinity of the Rio Grande Rise. The work included hydrographic and STD casts and current measurements.

In this study we examine with the historical data and these newer observations the characteristics of the waters that fill the southwestern Atlantic Ocean. We find, as other investigators have, several recognizably different layers. We attempt to identify these layers with their sources and to determine their mode of circulation.

We use two familiar concepts: 1) the large-scale flow is in approximate geostrophic balance, and 2) that flow and mixing take place principally along isopycnal surfaces. Combining these two we may expect to find that the depth variation of the isopycnals is defined largely by the sense and intensity of the geostrophically balanced large-scale circulation, and that the characteristics of the surface waters in an area are carried laterally along isopycnals that outcrop there, in the direction defined by the large-scale circulation and to the depths where the isopycnals must lie to maintain geostrophic balance.

A third concept used is that when waters from different sources are carried into the same area, their different densities may lead to a sharper vertical density gradient

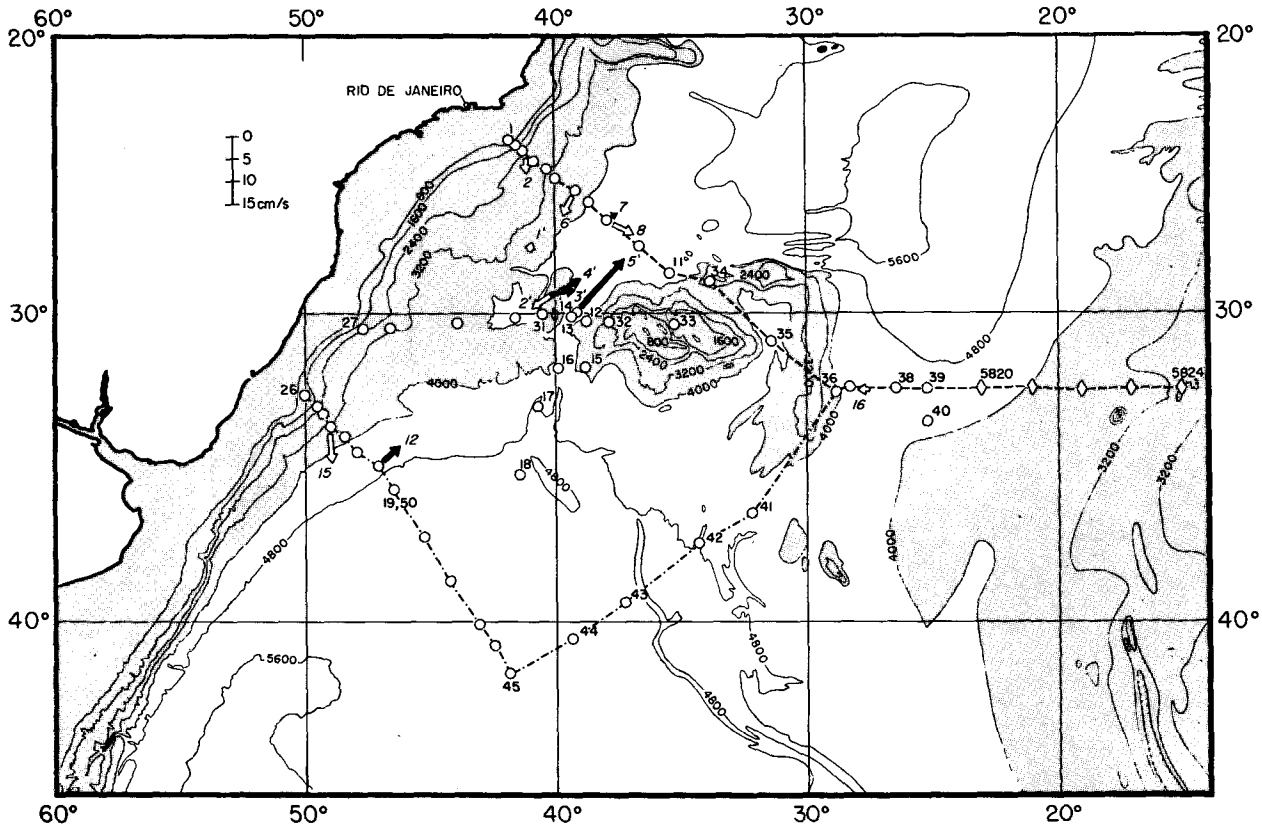

FIG. 1. Station positions of the Cato expedition 7 November–12 December 1972, and the five *Atlantis* stations, Cr. 247, that are used in the northern vertical section. The dashed line indicates stations used on the northern vertical section, the dashed-dot lines those on the southern line. Positions of current meters are indicated by italicized numerals. Black arrows indicate the currents measured at abyssal depths, and white arrows, the currents measured in the deep water.

at the interface than within either of the source waters. Such stability maxima are found to extend laterally over large areas and may provide useful clues to the origin and circulation of the various layers.

2. The water masses

The South Atlantic Ocean includes a vertical array of several recognizable layers of water. Each layer has originated from the surface waters in a particular area and has carried the characteristics of that area to the positions, appropriate to their density, where we observe them beneath the sea surface in the South Atlantic. Mixing between and along these layers, and biological activity, have modified the original characteristics, but some of the layers can be recognized over distances of thousands of kilometers.

Three vertical sections have been chosen to illustrate the characteristics. Two of the sections extend southeastward from the coast of South America to the Mid-Atlantic Ridge (Fig. 1) and the third extends from the northwestern Weddell Sea around the Scotia Arc and northward near the western boundary to 22°S (Fig. 2). This latter section was chosen to follow the northward extension of the densest waters that enter the South Atlantic Ocean from the Antarctic. As such, it cannot also represent ideally the southward flow of the deep water, which follows a path somewhat west of the section south to about 45°S but then turns eastward out of the section, or of the Antarctic Intermediate Water, which also diverges from this section.

The characteristics shown include potential temperature, salinity, oxygen, phosphate, nitrate, silicate,

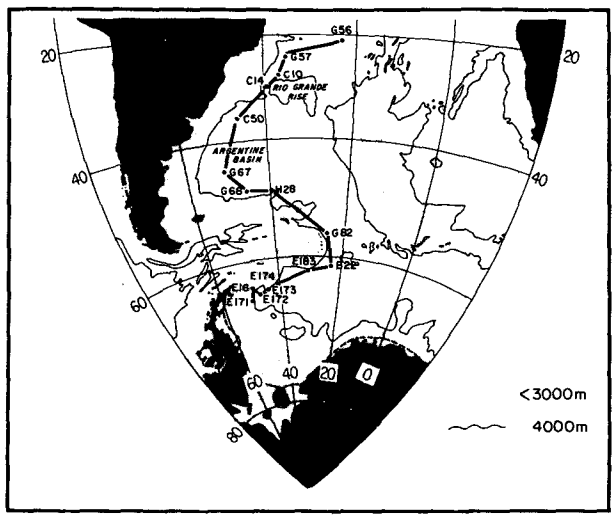

FIG. 2. Station positions along the north-south section. C indicates stations taken on the Cato expedition; G, GEOSECS Legs 5 and 6; H, *Hudson* Cr. 50; E, *Eltanin* Cr. 7, 12 and 22.

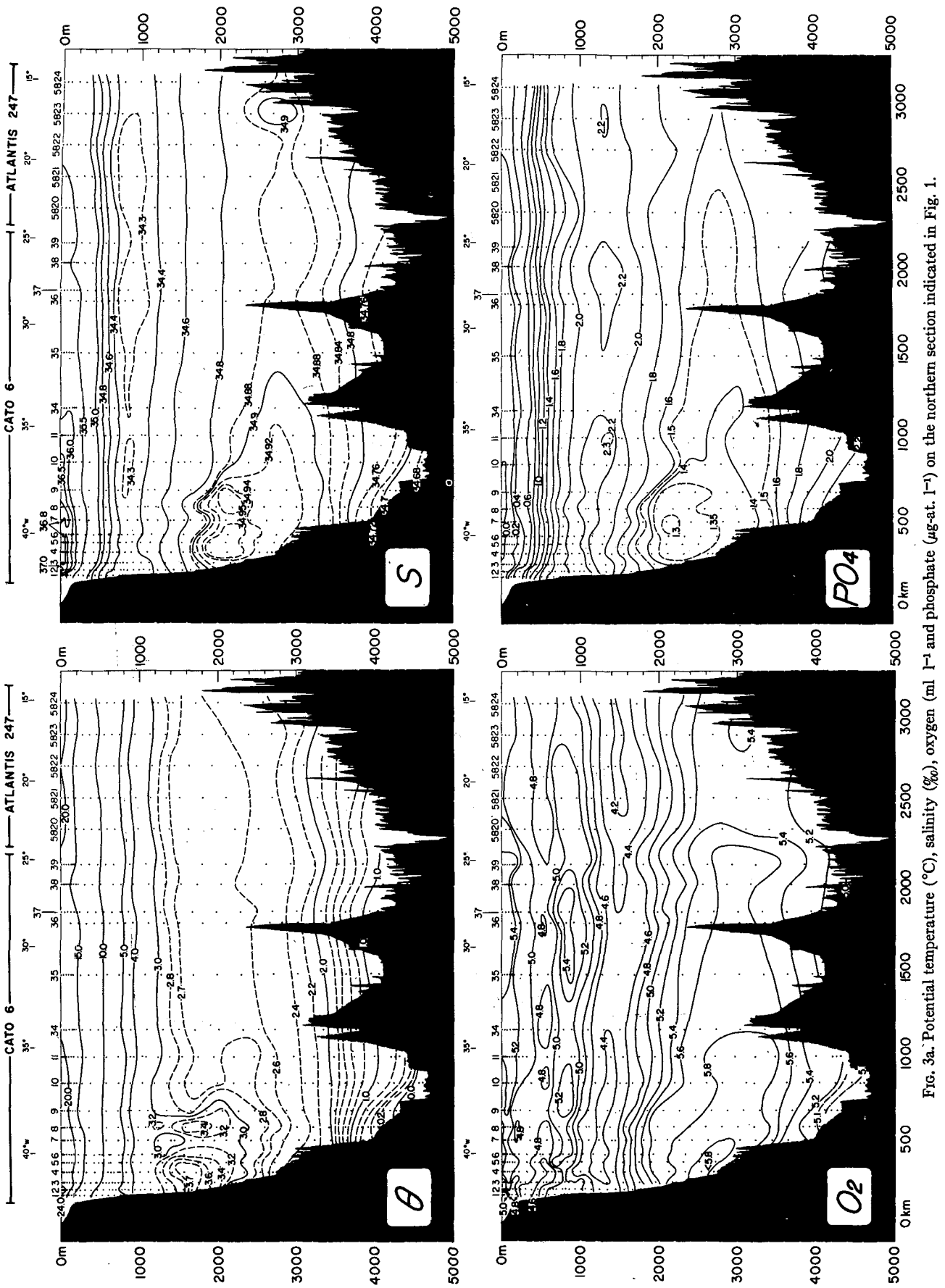

FIG. 3a. Potential temperature (°C), salinity (‰), oxygen (ml l^{-1}) and phosphate (μg-at. l^{-1}) on the northern section indicated in Fig. 1.

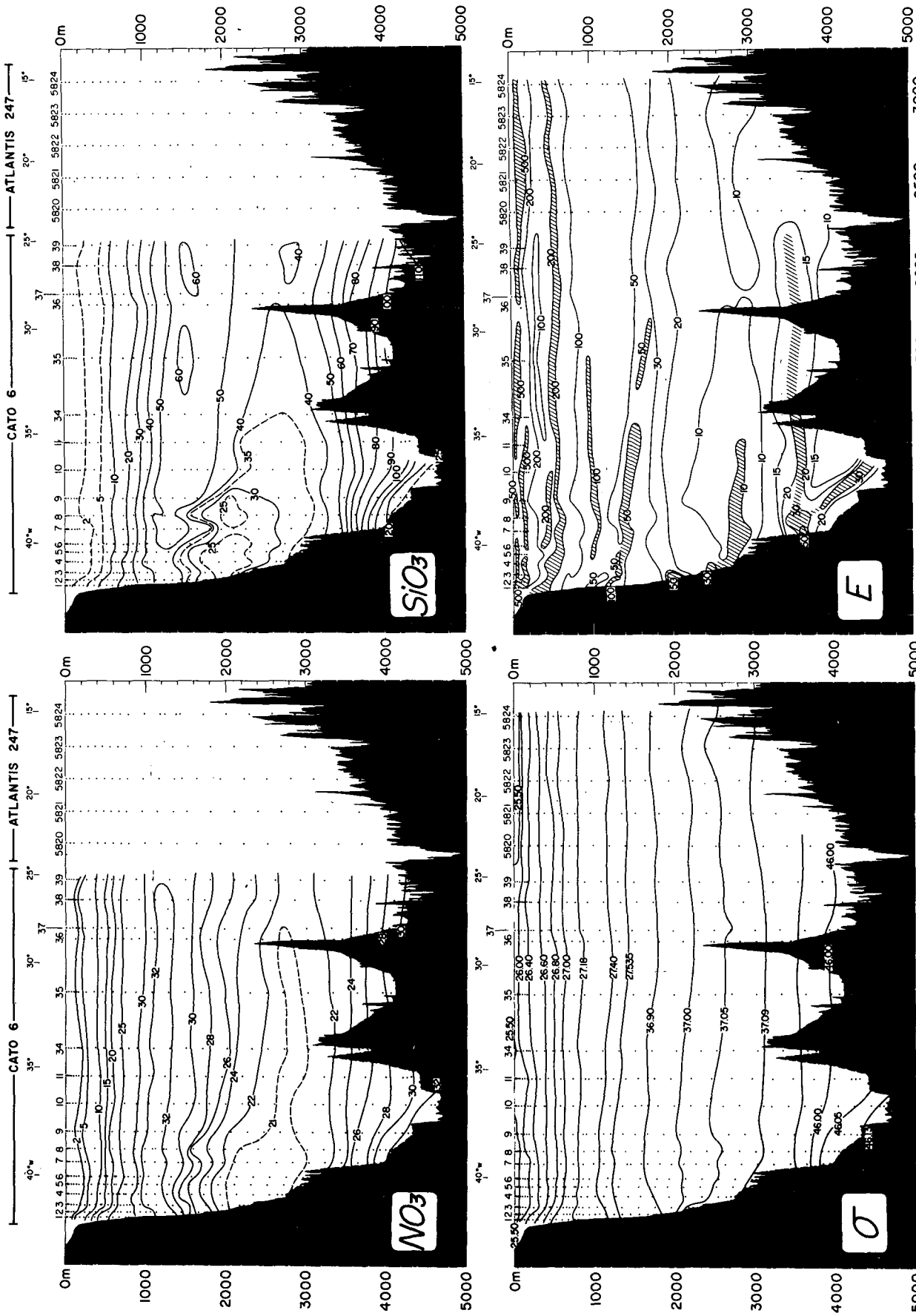

FIG. 3b. Nitrate (μg-at. l^{-1}), silicate (μg-at. l^{-1}), density parameter and stability (g cm^{-3} $m^{-1} \times 10^{-8}$) on the northern section indicated in Fig. 1.

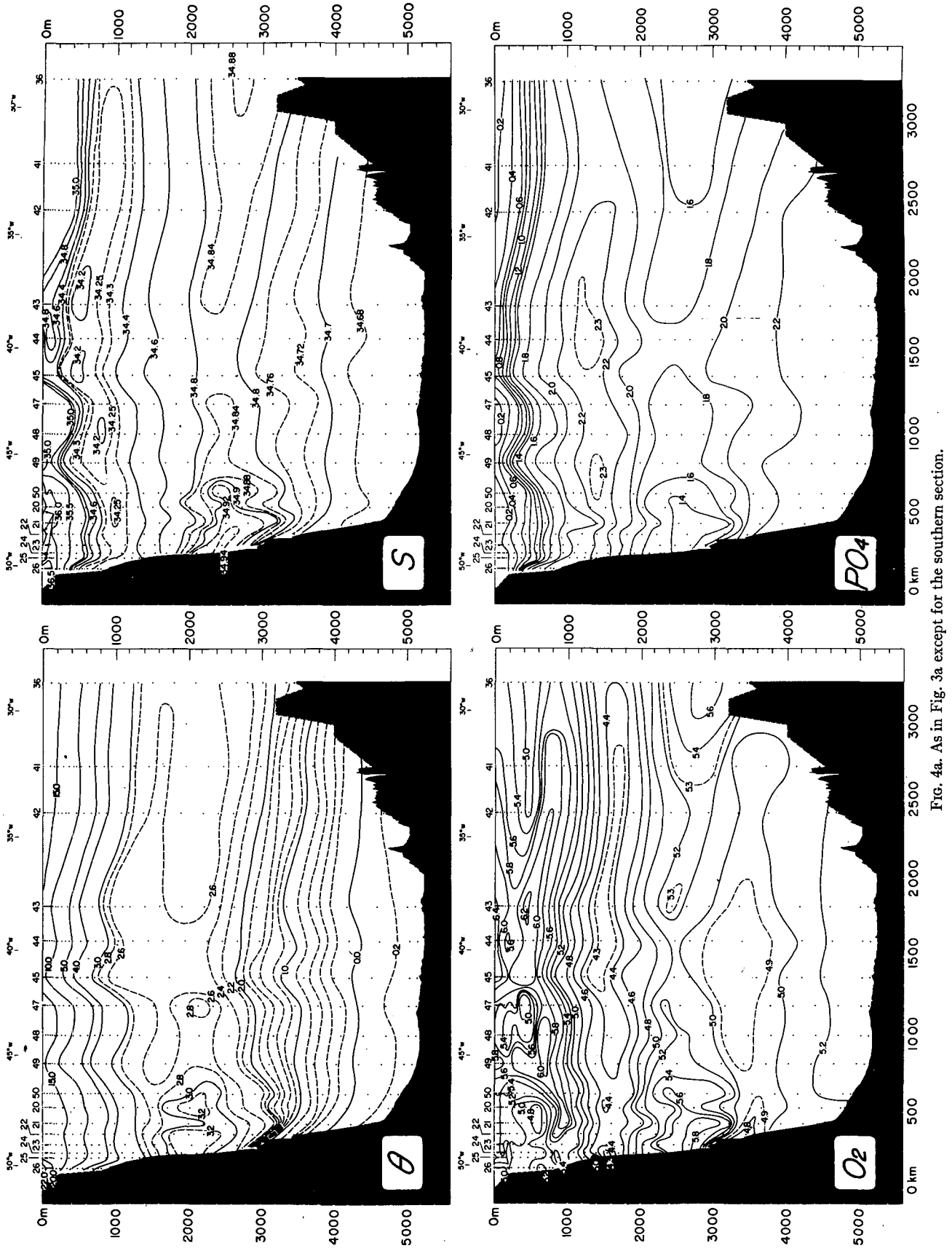

FIG. 4a. As in Fig. 3a except for the southern section.

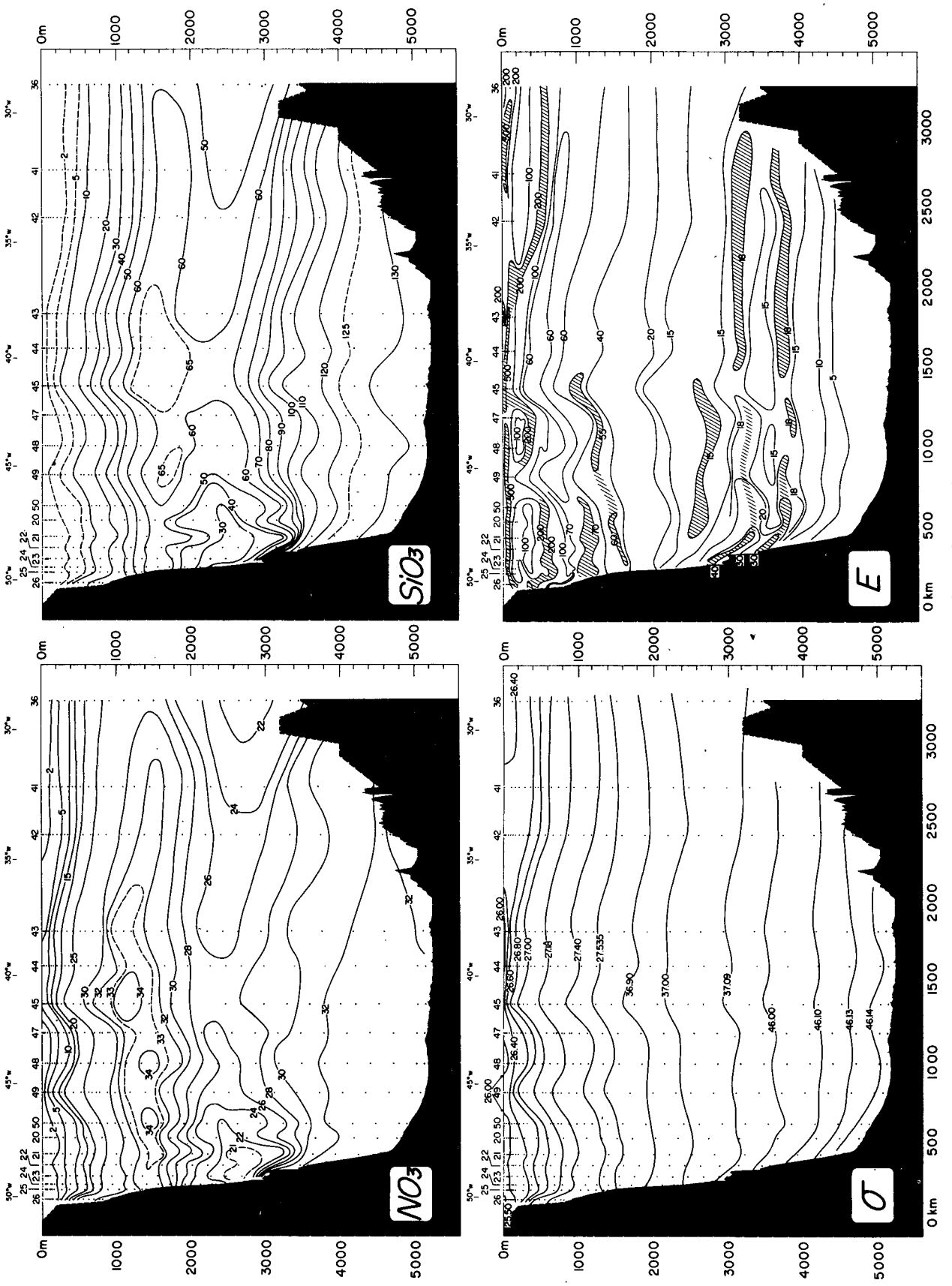

FIG. 4b. As in Fig. 3b except for the southern section.

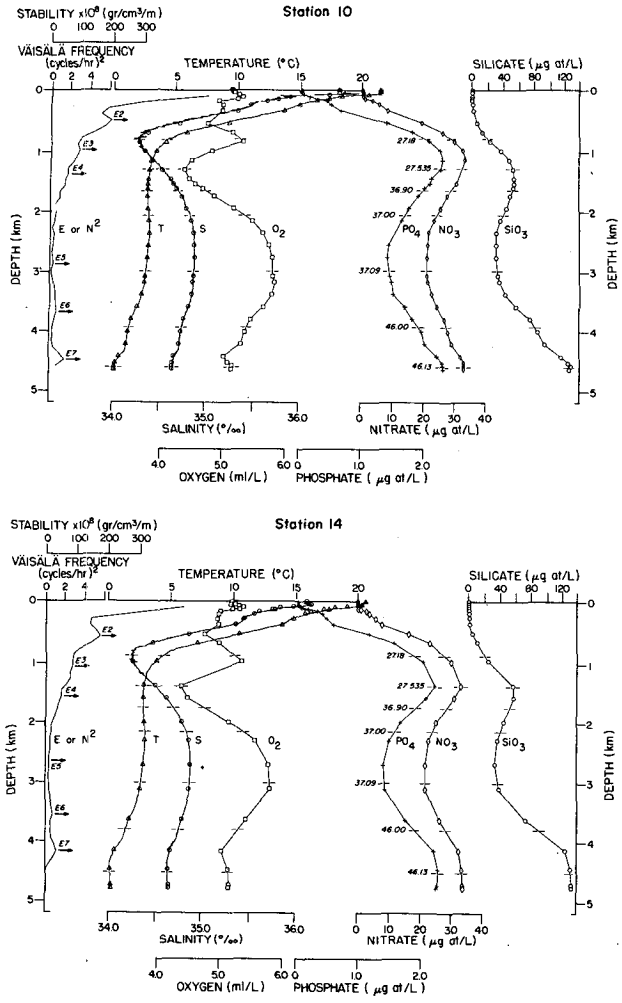

FIG. 5a. Profiles of characteristics at station 10 north of the Rio Grande Rise and station 14 in the deep channel through the Rise. Positions indicated in Fig. 1. The stability maxima are indicated by the arrows. The horizontal lines drawn through the profiles indicate the depth of the various isopycnal surfaces to be discussed later.

density, and hydrostatic stability. In the upper 1000 m the density parameter (σ_0) represents the density the water would have if moved adiabatically to the sea surface; between 1000 and 3000 m the parameter (σ_2) represents the density the water would have if moved adiabatically to a pressure of 2000 db, and below 3000 m the parameter (σ_4) represents the density if moved adiabatically to a pressure of 4000 db. The units are not ρ (g cm^{-3}) but $\sigma=(\rho-1)10^3$. The joining of density fields from one layer to the next is as in Reid and Lynn (1971) and will be illustrated in the figures. Hydrostatic stability (E) is in units of g cm^{-3} m$^{-1}\times10^{-8}$, as in Hesselberg and Sverdrup (1914).

a. The east-west sections

On the northern section (Figs. 3a, b), which lies just north of the Rio Grande Rise, there is a temperature maximum in the west between 1500 and 2500 m depth, and the coldest water is found in the western passage (the Vema Channel).

On the salinity section the highest values are at the surface. There is a salinity minimum near 1000 m with the lowest values toward the east, and there is a layer of high salinity with the highest values in the west, slightly below the depth of the temperature maximum. Below this salinity maximum the values decrease monotonically; the lowest values are found in the western passage.

The oxygen section shows low values in the pycnocline, a maximum layer near 800 m, just above the salinity minimum, and a minimum layer, with the lowest values in the east, lying between the salinity minimum and maximum layers. The oxygen maximum at about 2000–3000 m in the west is split near the western boundary by a small oxygen minimum (<5.8 ml l^{-1}, near 2500 m). The upper maximum lies below both the temperature and salinity maxima. Below the lower oxygen maximum the oxygen decreases to the bottom everywhere except within the western passage, where there is an increase near the bottom creating a minimum at about 4000 m.

The phosphate and nitrate patterns are quite similar. From the low values at the surface the concentrations increase to a maximum layer at about 1200–1400 m, nearly the same depth as the oxygen minimum. There is a minimum at about 2000–3000 m in the west, slightly below the salinity maximum and above the upper of the two deep oxygen maxima, and a monotonic increase to the bottom, with the highest values in the western passage.

Silicate is much like phosphate and nitrate, but the maximum layer at intermediate depth has its highest values toward the east, and the minimum, near 2000 m in the west, is slightly shallower than those in phosphate and nitrate: it appears to lie almost at the depth of the salinity maximum. The highest values are found in the western passage, at the bottom, below the deep oxygen minimum.

The characteristics on the southern section (Figs. 4a, b), which lies well south of the Rio Grande Rise, show much the same general features, with some notable differences. The temperature maximum and minimum are at slightly lower values and extend over a larger domain, considerably farther east than in the northern section, and the layer of colder abyssal water is much thicker. The salinity minimum is at lower values and lies somewhat shallower. The deeper waters have a single oxygen maximum, not separated by a small minimum along the western boundary as in the northern section at 2500 m. The deep minimum extends all the way to the Mid-Atlantic Ridge, with a thicker layer of higher oxygen beneath. The nutrient extrema are at higher concentrations.

These various maxima and minima in characteristics can be displayed on the profiles for selected stations. In Figs. 5a and 5b, vertical distributions of characteris-

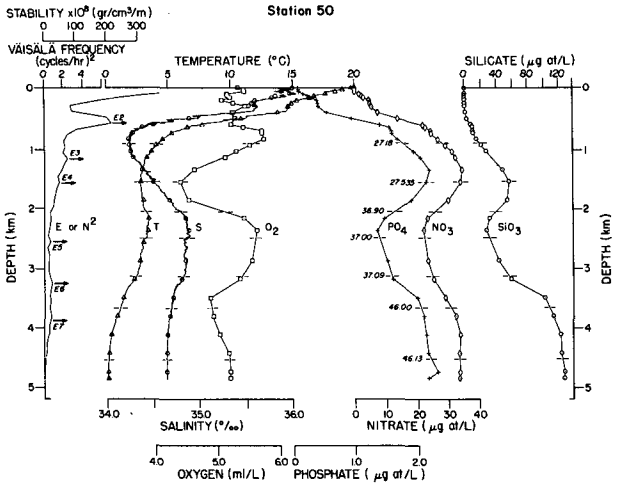

FIG. 5b. Profiles of characteristics at station 50 in the Argentine Basin. Position indicated in Fig. 1. The stability maxima are indicated by the arrows. The horizontal lines drawn through the profiles indicate the depth of the various isopycnal surfaces to be discussed later.

tics are shown for a station (10) in the Brazil Basin, a station (14) in the channel through the Rio Grande Rise, which separates the Argentine and Brazil Basins, and a station (50) in the Argentine Basin.

b. The meridional section

All of these features may be seen on the meridional section (Fig. 6), which extends farther south and includes some new features from higher latitudes. The subsurface temperature minimum, which was better developed on the southern section, is seen to extend into the Antarctic Circumpolar Current, and the lowest abyssal temperatures are seen within the Weddell Sea, beneath a sharp vertical gradient. The salinity minimum is seen to extend to the surface waters south of 50°S. The salinity maximum has its lowest value near 61°S; the maximum south of there must enter by another route.

The shallower oxygen maximum reaches the sea surface south of 45°S, and the underlying minimum is seen to extend across the Circumpolar Current into the Weddell Sea, but with a maximum value somewhere near 30° to 40°S. The minimum layer seen in the Circumpolar Current is split into two minima north of 50°S by the thick maximum layer extending southward from the North Atlantic. Near the bottom of the Weddell Sea there is a sudden sharp increase to very high oxygen values.

The nutrients have their maximum values at the bottom on both of the east-west sections, but southward from about 45°S the maximum layer is not at the bottom, but rises to the upper 2000 m within the Weddell Sea, with the highest values near 45°S and within the Weddell Sea separated by slightly lower values. Like temperature and oxygen, the nutrients change markedly near the bottom within the Weddell Sea.

c. Wüst's classification of layers

The extremes in salinity and oxygen have been used by Wüst (1935) to classify several layers. He identified the layer of low salinity at intermediate depths as originating from the surface waters of the subantarctic latitudes and called it Subantarctic Intermediate Water. Beneath the Intermediate Water he classified the thick high-salinity layer as North Atlantic Deep Water (NADW), and below that he called the colder, less saline layer the Antarctic Bottom Water.

He divided the North Atlantic Deep Water into three layers. He called the salinity maximum in the upper part of the layer Upper North Atlantic Deep Water, and he speculated that its source is the Mediterranean Sea. Beneath the salinity maximum he found two oxygen maxima and called these the Middle and Lower North Atlantic Deep Water (LNADW), and he stated that they originate from the Irminger and Labrador Seas, respectively.

d. Additional features

Wüst's (1935) gross classifications, based upon some of the salinity and oxygen maxima, leave some features unaccounted. He did not discuss the oxygen minimum that separates the oxygen maxima of his Middle and Lower Deep Waters. Also, the two major oxygen minima above and below the NADW do not belong either to the overlying Intermediate Water or to his Antarctic Bottom Water. And finally, the nutrient maxima near 1000 m depth within the Weddell Sea (Fig. 6—PO_4, SiO_3) had not been observed at the time of Wüst's (1935) study.

1) THE OXYGEN MINIMUM WITHIN THE NORTH ATLANTIC DEEP WATER

Possibly the reason Wüst (1935) did not discuss this layer is that he felt that low-oxygen values could be created by *in situ* consumption and that only the deep high values above and below required maintenance by advection or diffusion. Menzel and Ryther (1968), however, have proposed that oxygen consumption at such depths must be very low. We shall not attempt to account for this minimum, but only to show that it is a real feature.

Wüst (1935) indicated the presence of this deep oxygen minimum on all three of his meridional sections (Wüst, 1935: Beilagen XXIII, XXV, XXVII), and Wattenberg (1939) found it on the *Meteor* sections, but the minimum was only marginally detectable from their data over much of the area. Most of the more recent materials do not confirm its presence east of the Mid-Atlantic Ridge, though there is occasional evidence. This oxygen minimum can be seen all along

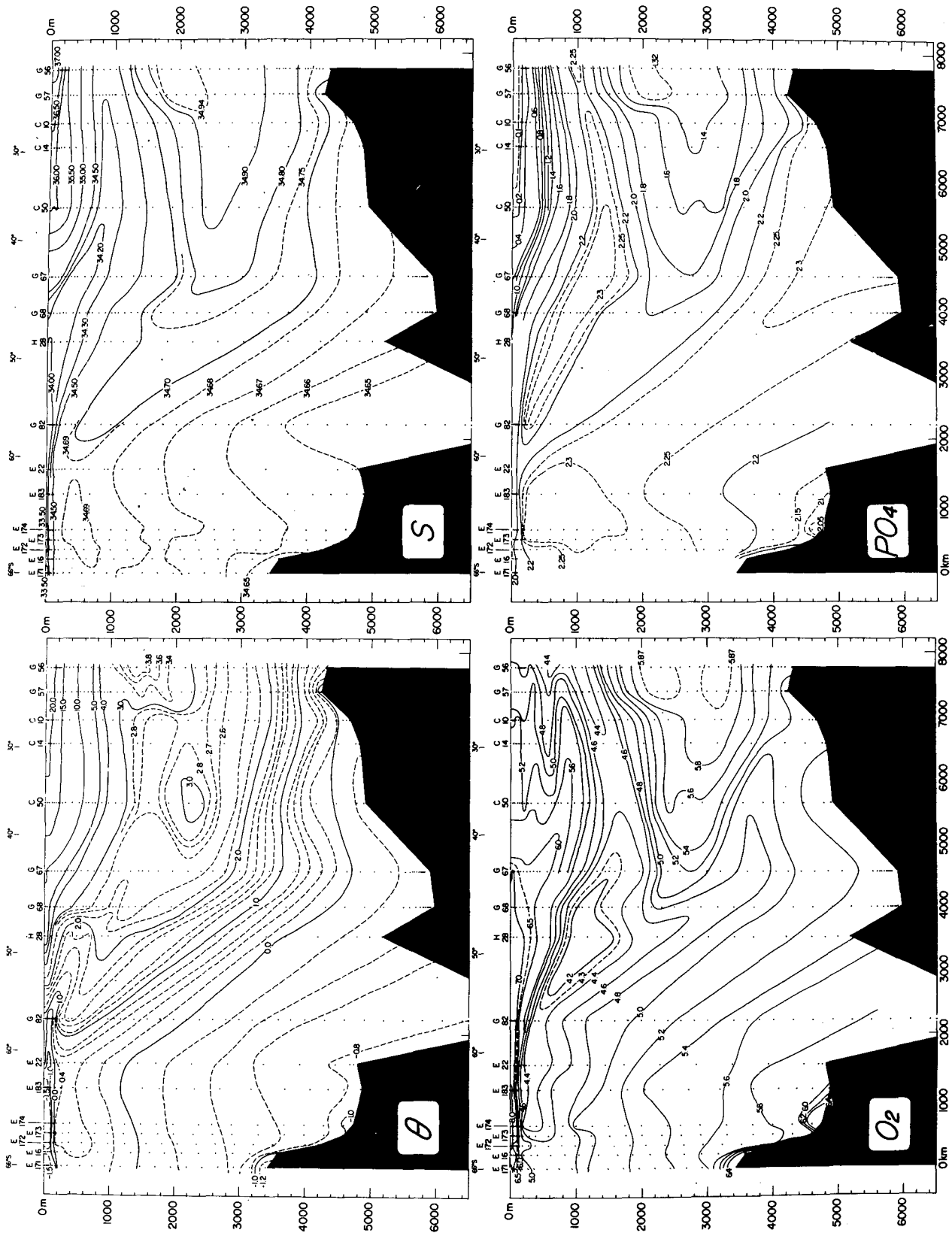

FIG. 6a. Potential temperature (°C), salinity (‰), oxygen (ml l^{-1}) and phosphate (μg-at. l^{-1}) on the north-south line indicated in Fig. 2.

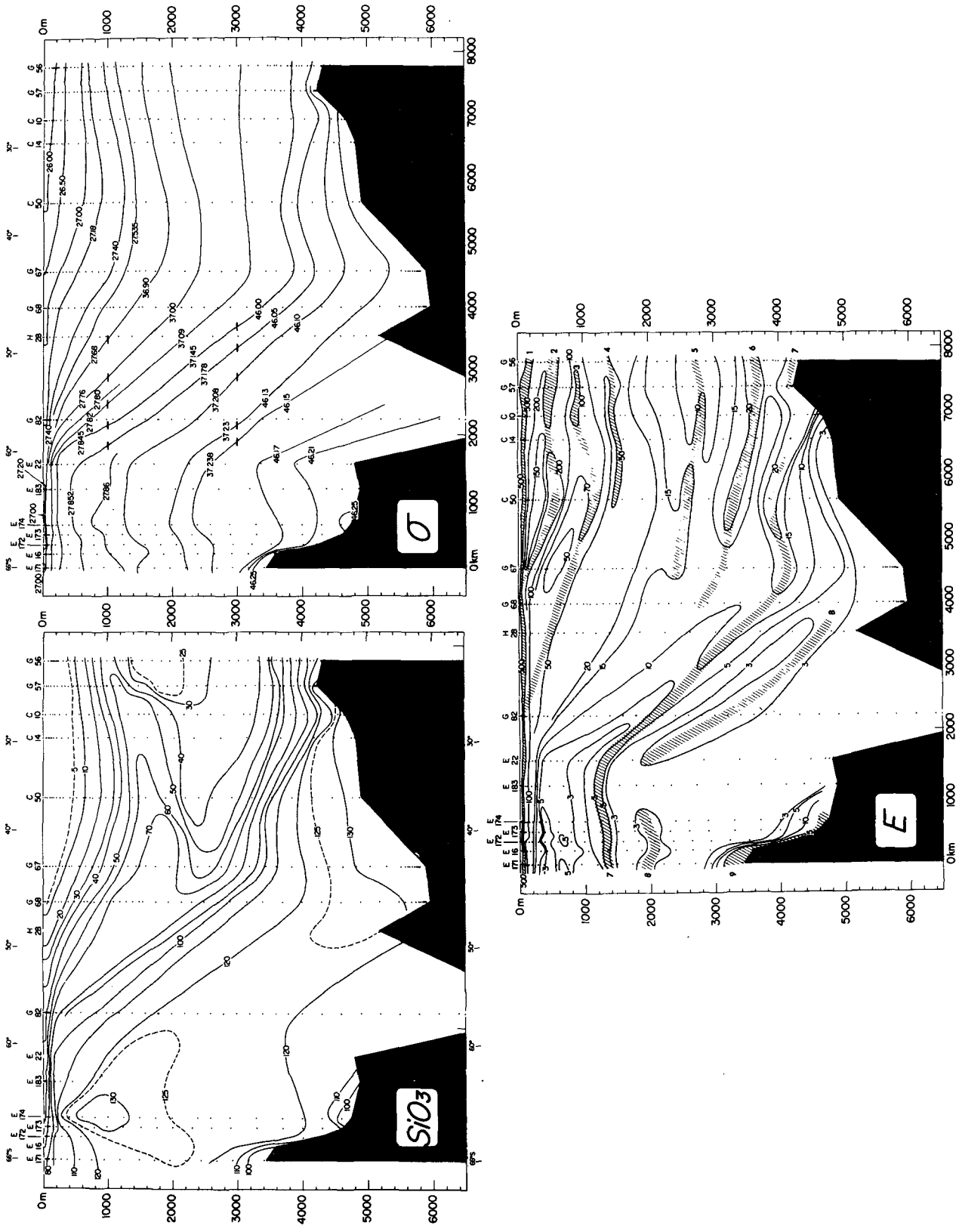

FIG. 6b. Silicate (μg-at. l^{-1}), density parameter and stability (g^3 cm^{-3} $m^{-1}\times10^{-8}$) on the north-south section indicated in Fig. 2.

the western side of the Atlantic Ocean, from the Labrador Sea (Worthington and Wright, 1970, Plate 57) all the way to the Rio Grande Rise in the various vertical sections prepared from the Gulf Stream '60 expeditions (Fuglister, 1963) and from the IGY expeditions of the *Atlantis*, *Crawford* and *Discovery* (Metcalf, 1958, 1959; Miller, 1960; Fuglister, 1957; Worthington, 1958). All three of Wüst's (1935) layers of NADW are evident on parts of the northern east-west section (Fig. 3a, Cato stations 3–7) and the meridional section (Fig. 6b, GEOSECS stations 56 and 57). The upper two can be seen also on the southern east-west section (Fig. 4a, Cato stations 20–23 and 47–50). The layers are also reported in the Brazil Basin near 8°S from 5° to 30°W by Edmond and Anderson (1971), who note a secondary salinity maximum very close to the deeper oxygen maximum in that area. They suggest that in that area the Upper Deep Water has maxima in both salinity and oxygen, the Middle Deep Water has minima in these characteristics, and the Lower Deep Water has maxima again. In the data north and south of their area, however, the salinity and oxygen maxima are not coincident but offset vertically; perhaps classifications based upon the core method lead to some confusion when the extremes in a conservative and a nonconservative characteristic are close together at one location but are separate downstream.

The absolute values at this oxygen minimum are about 6.4 ml l^{-1} within the Labrador Sea and about 5.8 ml l^{-1} near the Rio Grande Rise. The decrease at the minimum from north to south might be accounted for by lateral mixing with lower values to the east, which obtain all through the Atlantic north of about 40°S. Possibly the lowest value at the minimum is about 5.5 ml l^{-1} seen near 15° to 18°S in *Meteor* profile VI (Wattenberg, 1939).

2) The oxygen minima above and below the North Atlantic Deep Water and the nutrient maximum within the Weddell Sea

The single oxygen minimum seen on the meridional section south of 50°S lies very close to the temperature maximum and slightly above the salinity maximum. Sections of these characteristics across the Antarctic Circumpolar Current have been presented and discussed by Deacon (1937), Sverdrup *et al.* (1942) and Gordon (1967). This water, which is relatively warm and saline for high latitudes, has been called Circumpolar Water. Callahan (1972) emphasized the continuity of these characteristics around Antarctica and pointed out that the lowest values of oxygen at the minimum are found in the Pacific off the coast of Chile, and that the lowest oxygen values of this Circumpolar Water come from lateral exchange with the deeper waters of the Indian and Pacific Oceans. Its relatively high salinity, however, can derive only from the North Atlantic, but the high salinity of the Circumpolar Water south of 60°S is not continuous on the meridional section with the higher values to the north (Fig. 6a). Instead, the maximum in the south results from the cyclonic circulation within the Weddell Sea. It is illustrated on the isopycnal maps of Reid and Lynn (1971) and Callahan (1972).

From the meridional section of oxygen (Fig. 6a) it appears that north of 50°S the Circumpolar Water and the North Atlantic Deep Water meet [as Clowes (1933) has shown from the temperature-salinity characteristics] and that the oxygen maximum of the NADW splits the oxygen minimum of the Circumpolar Water into two separate minima. For the purposes of this investigation we refer to these layers as the upper and lower branches of the Circumpolar Water.

Within the Weddell Sea the oxygen minimum lies at about 400 m depth (Fig. 6a), and there are thick maxima in phosphate and nitrate just below the oxygen minimum (Fig. 6a, b). Gordon (1971a) has related the oxygen near 400 m depth within the Weddell Sea to the deep Pacific water entering through the Drake Passage. The density near the center of the nutrient maxima is about 27.86 in σ_0. This isopycnal extends into the deeper water at about 46.08 in σ_4. Within the Drake Passage and beneath the oxygen minimum and salinity maximum there is a silicate maximum very near the bottom, at about 46.08 in σ_4, and the silicate and phosphate values there are about the same as in the maxima within the Weddell Sea. It appears that it is this incoming Circumpolar Water, from the Pacific, that provides the high nutrient values found at 500–1500 m depth within the Weddell Sea.

3) The Weddell Sea Deep Water

Water of density greater than 46.10 in σ_4 is not found within the Drake Passage (Reid and Nowlin, 1971) and is therefore not part of the Circumpolar Water, but is formed within the Weddell Sea or farther east along the Antarctic Continent. This isopycnal lies below 4000 m depth in middle latitudes (Fig. 6c) and below 3000 m at the southern edge of the Drake Passage. Within the Weddell Sea it lies near 1400 m depth, immediately below the Circumpolar Water, which contains maxima in temperature, salinity, and nutrients and a minimum in oxygen (Figs. 6a, 6b). These characteristics change monotonically downward from the Circumpolar Water to the low values in temperature, salinity, and nutrients and the high oxygen values found in the newly formed bottom water of the Weddell Sea, at densities above 46.21 in σ_4 (Fig. 6c).

We shall refer to the layer beneath the isopycnal where σ_4 is about 46.10, and above the abyssal water of the Weddell Sea, with σ_4 greater than about 46.21, as Weddell Sea Deep Water.

4) WEDDELL SEA BOTTOM WATER

At the south end of the meridional section there is an abrupt decrease in temperature and in nutrient concentrations and a comparable increase in oxygen, reflecting the presence of the newly formed Weddell Sea Bottom Water (WSBW) (Figs. 6a, 6b). Carmack and Foster (1975) illustrated the distribution of temperature (and implicitly salinity) on an isopycnal surface ($\sigma_4 = 46.22$ below 3000 db) and found it moving eastward south of 60°S from its source, the western shelf of the Weddell Sea.

Carmack (1973) noted the abrupt cooling at the bottom and a comparable decrease in silicate below an overlying silicate maximum at ~1000–2000 m. He also suggested that the source of the silicate maximum might be local regeneration.

3. Stability

The hydrostatic stability does not decrease monotonically beneath the pycnocline, and we propose that the deeper stability maxima and minima may be related to the differences in density between the various water masses. Schubert (1935), using the *Meteor* data, detected several layers of maximum stability in the Equatorial and South Atlantic Ocean. Aside from the pycnocline, the principal and most laterally continuous maximum in stability that he found was near 1000 m depth in the middle latitudes of the South Atlantic, and he associated it with the lower boundary of the Intermediate Water. Boguslavskii and Koveshnikov (1965) noted that in the area near 15°S, 35°W, where they measured a northward flow at the salinity minimum, they observed a stability maximum at the lower boundary of the strong northward flow near 1000 m depth.

Schubert (1935) noted another maximum near 3000–4000 m in the South Atlantic, but it was not well defined by the *Meteor* data, and he made no suggestion as to its significance. More recently Reid and Lynn (1971) have shown similar deep stability maxima in the South Pacific and South Indian oceans. Craig *et al.* (1972) have described the South Pacific feature as a major vertical gradient in temperature (which they call a benthic front). Reid and Lonsdale (1974) have tried to relate the deep stability maximum in the western boundary flow to a shear zone between a northward-flowing bottom current of dense water and an overlying southward-flowing deep current of less dense water, but which the low-oxygen, high-nutrient waters return southward from the North Pacific.

Pingree and Morrison (1973) have related the position of the layer of Mediterranean Water between the Gulf of Cadiz and the Rockall Trough to a vertical minimum in stability, with maxima above and below.

In the station profiles (Figs. 5a, b) examples are shown of the hydrostatic stability (in g cm^{-3} m$^{-1}\times 10^{-8}$) or the square of the Brunt-Väisälä frequency (in cycles^2 h^{-2}). These stability values were calculated from STD data. Values of temperature and salinity were recorded in digital format at depth intervals of not greater than two meters, depending upon lowering speeds. These variables were averaged by depth intervals and used to calculate stability. In Fig. 7 the vertical profiles of temperature and salinity from the STD data, with bottle data superimposed, are shown for Cato station 14. Also shown are vertical profiles of stability calculated using T and S averaged vertically over a range of depth intervals (10, 20, 40, 70, 100, 200 and 400 m). For intervals of less than 20 m the results show features too thin to be followed laterally in our station spacing, even if they were assumed to be real and not time-dependent. At intervals from 20 to 40 m some features stand out more strongly, but beyond 100 m they tend to disappear. Pingree and Morrison (1973) reported somewhat similar results for the northwestern Atlantic Ocean. The stability values shown in Figs. 5a and 5b and in the vertical sections presented (Figs. 3b, 4b, 6b) were calculated using 100 m intervals below 1000 m and 40 m intervals above 1000 m.

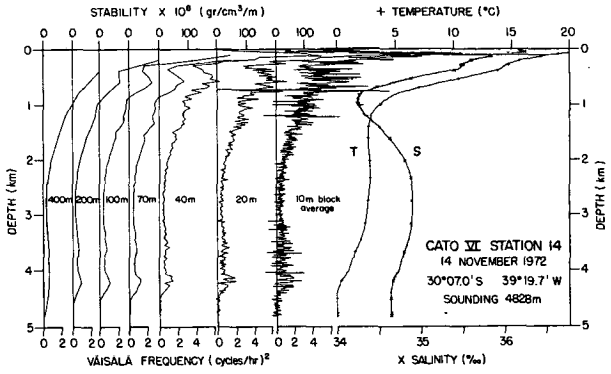

FIG. 7. Profiles of temperature and salinity (right-hand curves) from hydrographic casts and STD observations and the hydrostatic stability calculated from the STD records, averaging the T and S values over various intervals.

The maximum stability (Figs. 5a, b) is in the pycnocline, just beneath the surface layer, and reaches values so high (more than 500×10^{-8} g cm^{-3} m^{-1}) that it cannot be shown on the scale of these graphs. Below the pycnocline there is a decrease downward to about 2000 m. But the decrease is not monotonic; there are several maxima and minima in the upper 2000 m, and several more below 2000 m, where there is no general trend with increasing depth. The maxima lie near the inflexion points of the temperature and salinity profiles, as would be expected, and in some cases these are inflexion points in oxygen and nutrients, though these are not continuous traces and the depths of the inflexion points are not so clearly defined.

Of the various maxima the best defined are the shallow maximum (labeled 2) seen near 500 m (Figs. 5a, b), which lies just above the salinity minimum,

and the deep maximum (labeled 7) seen near 4500 m on station 10, 4200 m at station 14, and (weakly) at about 3900 m on station 50. Another maximum (labeled 3), near 1000 m on station 10 and 1200 m on station 50, is well defined on most of the stations: this is the feature that was clearest in Schubert's (1935) results. Number 6 is clearest in the northern and western Cato stations. Numbers 4 and 5 are clear in some cases in the north, but marginal or missing in others. From the few clear cases, we conjecture that they are real features, though not always evident in the present array of data.

These various stability strata can be recognized also in most of the hydrographic stations in spite of the limited resolution provided by the vertical sample spacing. Figs. 3b and 4b show the stability features on east–west lines along about 30°S and about 40°S. The same figures show the distributions of potential density along these sections. The stability features can be identified on these east-west sections, but it will prove more illuminating to examine them on the north-south section (Fig. 6b) which gives some indication of their origins. This section was chosen to represent the path of flow of the deepest water, but it will, of course, cut across the Antarctic Circumpolar Current and the upper flow of the subtropical anticyclonic gyre. Fig. 6b shows the density on this north–south section and emphasizes the strong upward slope of the isopycnals to the south across the Antarctic Circumpolar Current, and the moderate slope upward to the north beneath the northern limb of the anticyclonic gyre.

The distribution of stability is shown in Fig. 6b with the layers of maximum values hatched. There are several of these layers, and explanations are offered for most of them. The stability stratum labeled 1 is, of course, the main pycnocline. The next two strata, 2 and 3, encompass the salinity minimum which characterizes the Intermediate Water. This can be seen on the vertical sections and on the profiles (Figs. 5a, b). Between the third and fourth lies a layer of lower oxygen and higher phosphate and nitrate; the silicate maximum lies at or below the fourth stratum on some stations. The fourth and sixth strata encompass the salinity and oxygen maxima and the nutrient minimum of the North Atlantic Deep Water; the fifth stratum lies within the NADW and may separate some of the sublayers that Wüst discussed. At station 50 (Fig. 5b) there is a clear break in the temperature and salinity profiles there, and at the northern end of the meridional section the fifth stratum lies near 2800 m, just below the temperature and salinity maxima and nutrient minima of the NADW, and in the weak oxygen minimum.

Our sixth stratum lies slightly deeper than the 2°C potential temperature that Wright (1970) chose as an approximate upper boundary in his study of the northward transport of the Antarctic Bottom Water. His choice was based partly on a break in the θ-S curve as described by Worthington and Metcalf (1961). We find the maximum vertical gradient of potential temperature (and hence the stability maximum) from about 1.4° to 2.0°C (potential temperature) near the western boundary, but at lower temperatures, from about 1.2° to 1.8°C, in the eastern part of the sections. The sixth and seventh strata encompass an oxygen minimum that appears to derive from the Circumpolar Water, and the seventh may be the separation between the water that has entered the Atlantic via the Drake Passage and the denser water of Atlantic (Weddell Sea) origin. The eighth we do not understand.

The ninth stability stratum is found only in the far south where it separates the newly formed Weddell Sea Bottom Water from the overlying Weddell Sea Deep Water (Carmack and Foster, 1977).

4. Circulation

The circulation of the South Atlantic Ocean includes a large subtropical anticyclonic gyre roughly similar to those seen in other oceans. It consists of the South Equatorial Current, the Brazil Current, part of the Antarctic Circumpolar Current, and the Benguela Current. The east-west axis of the subtropical gyre is near 25°S at the surface, but at greater depths it appears farther south: at 3000 m depth the axis lies near 45°S, as can be seen also from the maps of Montgomery and Pollak (1942). South of this anticyclonic gyre the Falkland Current extends northward from the Scotia Sea to about 40°S along the coast of South America and then turns eastward as part of the subtropical gyre.

From consideration of the vertical shear calculated from the geostrophic approximation and of the characteristics and sources of the various water masses, we present a qualitative but coherent scheme of the deeper circulation of the southwestern Atlantic Ocean. The patterns of circulation that we will use throughout this discussion are represented by the various maps of relative geopotential anomaly, or geostrophic shear (Figs. 8–11). The general circulation of the surface waters for the entire open Atlantic is represented by Fig. 8. Because the Brazil Current flows mostly over depths of less than 2000 m, it is not well represented on this map. This is true also for the inshore part of the Gulf Stream and other major currents over the broad shelves of the northern North Atlantic Ocean such as the Norwegian and Labrador Currents.

In the South Atlantic Ocean there is a high in geopotential anomaly near the western boundary, present over all of the pressure intervals, though the latitude of the highest values lies farther poleward on the deeper maps. In the near-surface layers we take this high to represent a subtropical anticyclonic gyre, with its center so far toward the west that there is an equatorward return flow just offshore from the poleward flow. A comparable feature is seen in the 2.0 and 2.2 contours

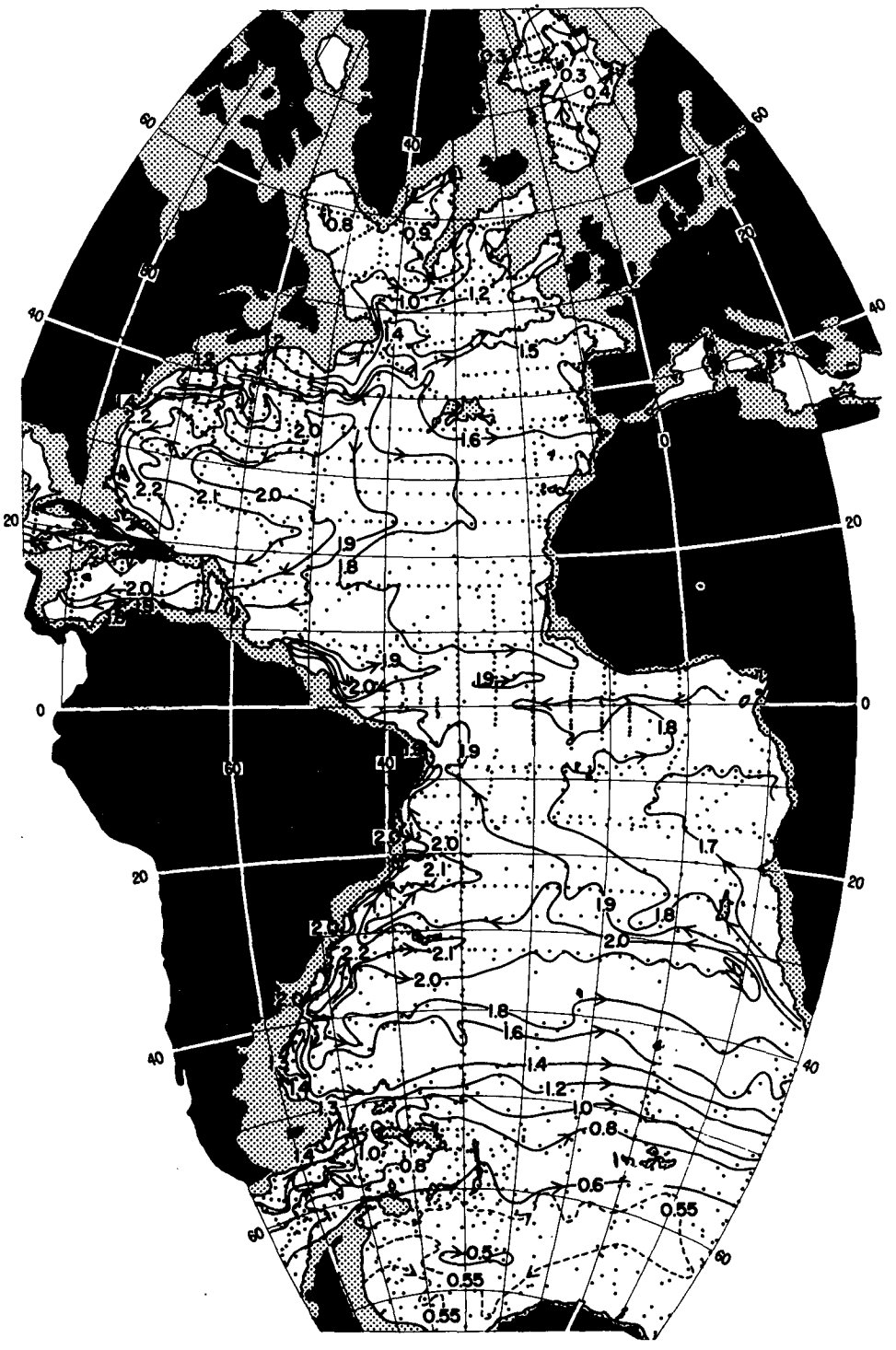

FIG. 8. The geopotential anomaly at the sea surface with respect to 2000 db in dynamic meters (10 J kg^{-1}).

at the latitude of the coastal part of the Gulf Stream (25°–35°N).

A subtropical high cell, with an equatorward geostrophic shear on the eastern side of the high, has appeared in all maps of the density field of both the Gulf Stream (Iselin, 1936; Defant, 1941) and the Brazil Current (Defant, 1941; Buscaglia, 1971), though the data available to Defant were not sufficient to show it very clearly. It is quite clear in the corresponding near-surface maps for the Kuroshio and East

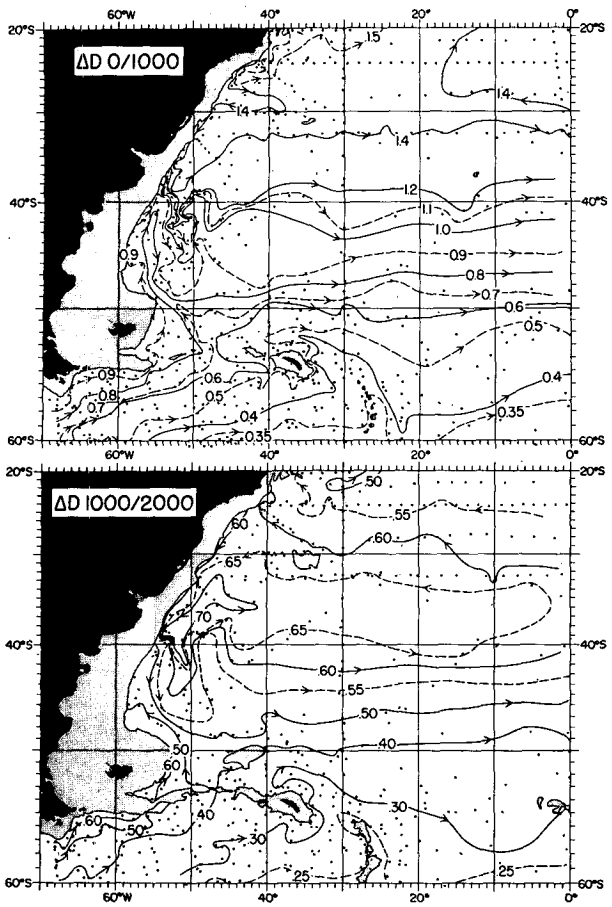

FIG. 9. (upper) The geopotential anomaly at the sea surface with respect to 1000 db in dynamic meters (10 J kg^{-1}). (lower) The geopotential anomaly at 1000 db with respect to 2000 db in dynamic meters (10 J kg^{-1}).

Australia Currents (Reid, 1961; Wyrtki, 1975; Hamon, 1970) and is seen to extend to 3500 m depth in the Pacific (Reid and Arthur, 1975).

Note that this sort of offshore return is seen also for the Falkland Current. Like the Brazil Current, this current lies mostly in water too shallow to be revealed fully by the 0/2000 db map (Fig. 8) and is seen better at 0/1000 db (Fig. 9). In both cases the flow turns sharply back again before turning eastward as the southern limb of the anticyclonic gyre. The 0/1000 db map for the southwestern Atlantic Ocean extends farther toward the western boundary and shows the Brazil Current somewhat more clearly. This current extends southward along the coast to about 40°S, continues farther southward offshore of the Falkland Current, and then turns eastward as part of the subtropical anticyclonic gyre.

At 1000/2000 and 2000/3500 db (Figs. 9 and 10) there is clearly a southward shear along the western boundary. We shall (perhaps arbitrarily) call the southward flow above about 1000 db the Brazil Current and assume that the deeper water, with its salinity, temperature and oxygen maxima, is of separate origin.

We have interpreted the high in geopotential anomaly as evidence of anticyclonic shear, which appears to extend to great depths. North of 40°S the shear along the western boundary is poleward at all depths relative to the bottom flow. But the characteristics of the abyssal waters at the boundary indicate that these waters have come from farther south. It follows that the sense of flow must change at some depth between the deep water of northern origin, flowing southward, and the underlying water of southern origin, flowing northward. While there is no reason to believe that this change in sense of flow takes place at the same depth everywhere in the area, or that we can identify it precisely, we may at least recognize that the shift occurs and keep this in mind when examining the maps of geostrophic shear. Therefore, we represent the abyssal flow by the map of geopotential anomaly at 4000 db relative to 3500 db (Fig. 11); we assume that north of 50°S this reference will provide the correct sense of flow for those waters that lie substantially shallower or deeper than 3500 m, but at depths near 3500 m the sense of flow is, of course, not well determined. South of 50°S in the Antarctic Circumpolar

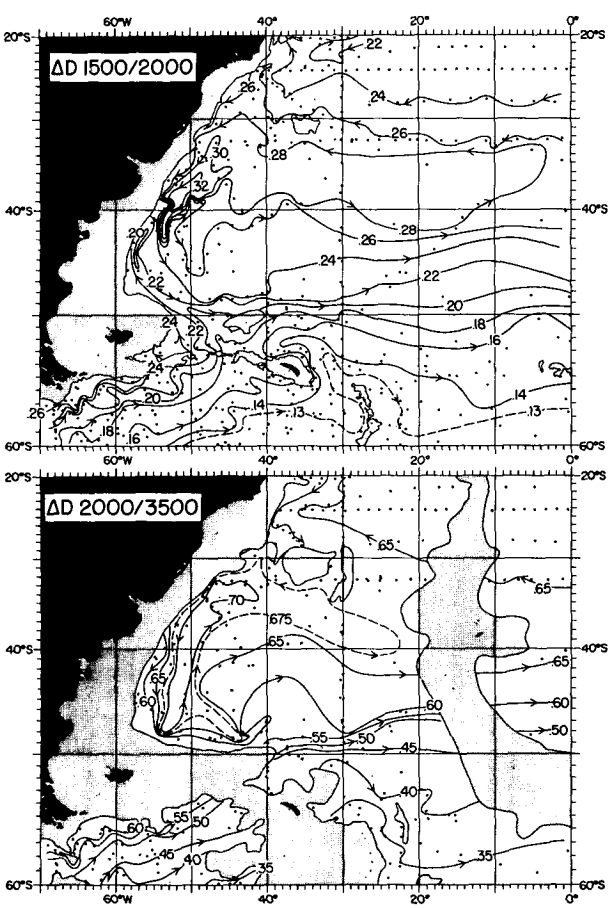

FIG. 10. (upper) The geopotential anomaly at 1500 db with respect to 2000 db in dynamic meters (10 J kg^{-1}). (lower) The geopotential anomaly at 2000 db with respect to 3500 db in dynamic meters (10 J kg^{-1}).

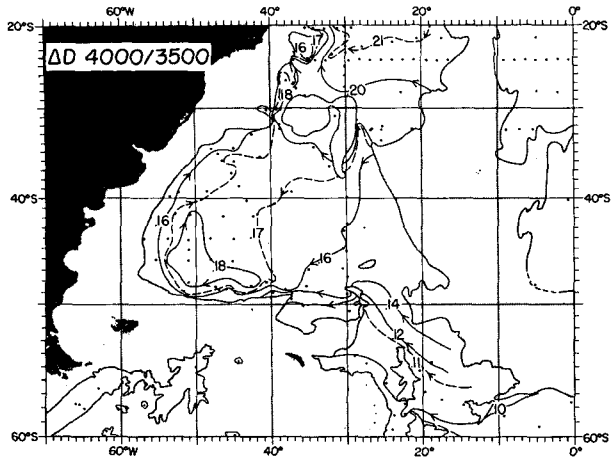

FIG. 11. The geopotential anomaly at 4000 db with respect to 3500 db in dynamic meters (10 J kg^{-1}).

Current the geostrophic shear might require quite a different sort of reference in order to be useful. We note that the 3500 db surface is 1000 to 2000 m below that suggested by Defant (1941) for this area and used by Wüst (1957).

Stommel (1958a) and Stommel and Arons (1960a), found cyclonic flow in the abyssal layers of the Atlantic, Pacific and Indian Oceans but showed only poleward flow along most of the western boundary of the South Atlantic. This was because the simplified model allowed abyssal flow in only one direction at each location. Thus, the equatorward flow of Antarctic Water beneath the water from the North Atlantic could not be accommodated along the entire western boundary of the South Atlantic, although its existence was, of course, recognized.

The principal meridional flow of the waters with which we are concerned takes place near the western boundary. Except within the abyssal layer, the flow is southward along the western edge of the subtropical anticyclonic gyre (Figs. 8–11), and the waters not only turn eastward near 40°S, but some part of them also recirculates around the gyre. Shallow waters also enter from the south and move northward along the western boundary to about 40°S, where they also turn eastward as part of the gyre, and some part of them also extends northward along the eastern side of the gyre.

The meridional flow of the abyssal waters also takes place along the western boundary, and the density field may be taken to indicate that this flow includes a cyclonic gyre. Ewing *et al.* (1971) found evidence of the abyssal equatorward flow in the sediments of the Argentine Basin. The northward flow of the abyssal waters takes place somewhat east of the southward flow of the deep waters because of the broad continental slope off South America. The horizontal distance from the 2000 m isobath to the 4500 m isobath varies from about 150 to 350 km in the latitudes south of the Rio Grande Rise. Some distinction between the flow of these two layers has been found by Burckle and Stanton (1975) in the sediments: antarctic diatoms appear only on the lower parts of the continental slope offshore (below 2000 m) in the Argentine Basin.

5. Current measurements

During the Cato expedition and later during *Chain* cruise 115, Leg 6 (Johnson *et al.*, 1974), several deep

TABLE 1. Current measurements.

No.	Latitude (°S)	Longitude (°W)	Between or at stations	Corrected sounding (m)	Meters off bottom	Depth (m)	Total hours	Mean vector Direction (°T)	Mean vector Speed (cm s^{-1})
Cato 6									
2	24°32.8′	41°02.3′	3–4	2714	200	2514	642.5	183°	3.3
3	25°15.2′	39°59.2′		3080	200	2880	4.5	164°	5.8
4	25°15.2′	39°59.2′		3080	1000	2080	4.5	210°	8.8
6	25°47.4′	39°24.3′	7	3918	1000	2918	688.5	206°	5.0
7	26°45.8′	37°59.3′	9	4370	200	4170	743.0	065°	0.9
8	26°45.8′	37°59.3′	9	4370	1000	3370	739.5	119°	5.5
9	28°07.7′	36°06.4′		4413	1000	3413	6.5	190°	2.5
9′	28°07.7′	36°06.4′		4413	1000	3413	22.5	026°	3.8
10	30°08.6′	39°23.2′		4845	200	4645	2.0	033°	21.7
12	35°10.8′	47°03.9′	20	4819	200	4619	494.5	050°	5.4
13	34°37.5′	47°59.0′		4522	1000	3522	478.0	350°	21.2
15	33°43.0′	49°02.0′	23	3016	800	2216	238.0	175°	6.8
16	32°30.0′	27°39.2′		4174	1000	3174	48.5	269°	2.7
Chain Cr. 115, Leg 6									
1	27°49.0′	40°59.5′		2972	1000	1972	454.0	015°	2.4
2	29°20.2′	40°05.0′		4304	1000	3304	426.0	236°	5.7
3	29°20.1′	40°05.1′		4320	10	4310	424.5	079°	5.7
4	29°22.2′	40°07.5′		4288	10	4278	422.5	059°	7.8
5	30°10.8′	39°22.7′	13–51	4933	10	4923	373.0	043°	14.8

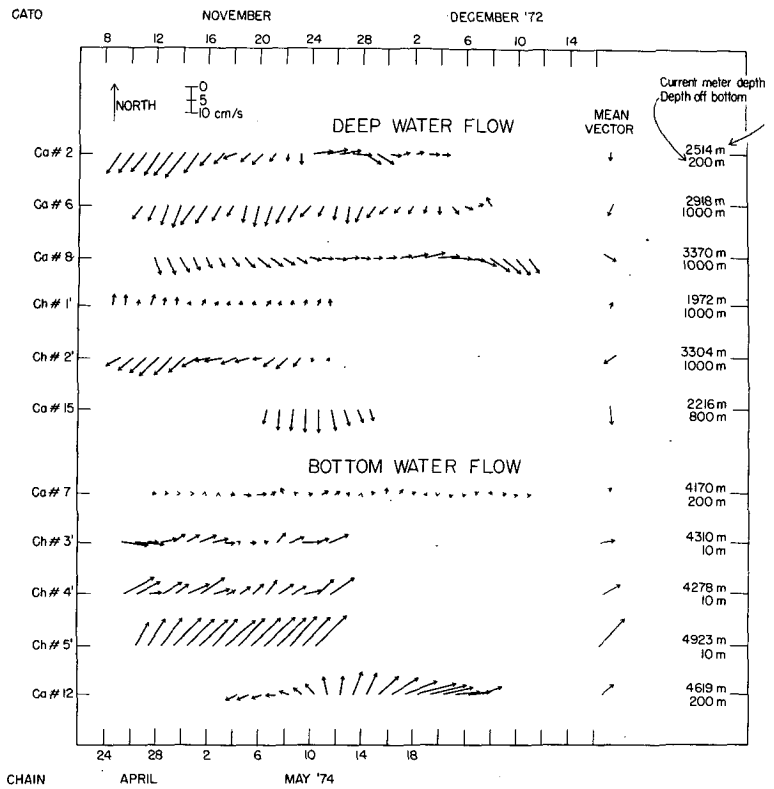

FIG. 12. Daily mean velocity vectors for the 11 current records that were longer than 200 h. Cato records are indicated by Ca and *Chain* records by Ch.

current meter records were obtained to the north and south of the Rio Grande Rise, as well as in the Vema Passage through the Rise (Fig. 1 and Table 1).

The expeditions were each carried out in a few weeks and no long-period deployments could be made. The positions of the meters were chosen to test the general hypothesis of poleward flow of the deep waters along the western boundary and equatorward flow of the abyssal waters. We conjectured that the abyssal flow might be strongest in the deep channel through the Rio Grande Rise and that measurements there might give useful information about the major flow, even in the presence of the variability to be expected.

Table 1 lists the current measurements. The current meters have been described by Sessions (1975). They are of the type used by Reid and Nowlin (1971) in the Drake Passage and by Reid and Lonsdale (1974) in the Samoan Passage. They sense speed and direction by a Savonius-rotor and a vane, record internally, and are deployed as bottom-moored, subsurface arrays, with timed anchor releases. Some of the Cato current meters (1, 3 and 4) were dropped for only a few hours to provide some estimate of the ambient velocity for planning the other deployments. Others gave only short records (9, 10) or did not function properly (11, 14) and one (5) was not recovered. Semidiurnal variations of about 2 cm s^{-1} amplitude are present in all of the records. The daily mean velocity vectors for the 11 records longer than 200 h are shown in Fig. 12. Most of these show substantial variability. Cato records 2 and 12 show the greatest variability and *Chain* record 5 the least.

a. Measurements in the Deep Water

Current measurements at Cato moorings 2, 6, 8 and 15 and *Chain* moorings 1 and 2 were at depths within the NADW (1907 to 3370 m), and all except *Chain* 1 recorded southward flow (Fig. 12). *Chain* mooring number 1 recorded a northward flow but at lower speed. Cato mooring 16, in the deep trough east of the Rio Grande Rise, could be deployed for only 48 h. From the water characteristics we did not expect a high velocity so far east, and this brief record shows quite low speed.

b. Measurements in the Bottom Water

Measurements at Cato moorings 7 and 12 and *Chain* moorings 3, 4 and 5 were at either 10 or 200 m off the bottom in depths from 4162 to 4809 m (Table 1). Cato 12 was located in the northwestern Argentine Basin in the anticipated path of northward-flowing bottom water (Fig. 11). Farther north, *Chain* 5 was located in the southern entrance of the Vema Channel, the only connection for the bottom western boundary current passing from the Argentine to the Brazil Basin. The resulting daily velocities are the steadiest and highest of all the records. Farther north, the Vema Channel

becomes shallow and splits into two branches. The *Chain* 3 and 4 current measurements were made in these western and eastern channels leading to the Brazil Basin. Although these records have more variability than the *Chain* 5 record, they indicate consistent flow confined by the local bathymetry into the Brazil Basin. Current record Cato 7 was located north of the Rise along the western margin of the Brazil Basin and, though the resultant vector for 31 days was towards 65°N, the flow was very weak and quite variable.

When viewed individually, the 11 deep and bottom current measurements show strong variability. However, when these records are viewed in the context of the distributions of characteristics, they support our conjectures about the large-scale circulation. In addition, they give at least for a few points and a short time a measure of the actual velocity field that the other data cannot provide.

6. Vertical sections of geostrophic shear

Some inferences about the meridional flow can be made from the density field, particularly near the western boundary, where the flow is stronger and the isopycnals slope more steeply.

On the northern section (Fig. 3b), the density field west of station 6 suggests a poleward shear below 2000 m relative to 3000 m, weakening or reversing above 2000 to about 1000 m, and strengthening upward above 1000 m. Between stations 7 and 11 there is a poleward shear relative to the bottom up to about 3500 m, and little shear upward from there. Eastward from station 11 the isopycnals are nearly level, and the shear is weak.

West of station 6 the characteristics indicate the presence of the Brazil Current, which must be flowing poleward, above 1000 m, and the NADW, which is also flowing poleward, between 1500 and 3000 m. A reference flow of zero at 3000 m would give poleward flow everywhere in the NADW and the Brazil Current, and a weaker poleward flow (or possibly an equatorward flow) between 1000 and 1500 m.

Antarctic characteristics are present below 3500 m between stations 7 and 11. A reference flow of zero at the bottom would yield poleward flow below 3500 m. We assume, then, an equatorward flow at the bottom, decreasing upward to about 3500 m.

Roughly the same pattern is seen on the western part of the southern section (Fig. 4b), allowing for the difference in the continental slope, but in the central part of the section the isopycnals vary more in depth, reflecting the sinuous flow around the southern limb of the anticyclonic gyre.

It seems useful to calculate the relative geostrophic velocity fields for these two sections and compare them with both the observed currents and the previous large-scale interpretations. The results depend upon the depth or velocity chosen as reference. It is reasonable to assume from the characteristics above and below stability layer number 6 that it separates the equatorward-flowing bottom waters from the poleward-moving deep waters; this gives much the same reference that Wright (1970) used. Thus, we have chosen this stability maximum as our reference depth for both Cato sections (Figs. 3b and 4b). It intersects the bottom just east of stations 6 and 24 on the northern and southern lines, respectively, and a new reference must be selected for the western part of the sections. Near 1000 m in both sections the isopycnals diverge near the continental slope. Depending on the reference level selected, this will yield either northward flow or weaker southward flow between 1000 and 1500 m. From the shear maps (Figs. 9 and 10) we note that the anticyclonic gyre includes (relative) flow across the northern section that is northward east of station 5, turning back across the section southward between station 5 and the coast. Likewise, for the southern section, the maps show a (relative) southward flow west of stations 20–21 and a northward return flow of stations 20–21, as discussed in the section on circulation. We choose the third stability stratum as a reference in the shallower western area.

The fields of relative velocity that result from the choice of stability layer number 6 as a reference for the offshore station pairs and stability layer number 3 as a reference for the nearshore stations pairs are given in Fig. 13. (These calculations can extend downward, of course, only to the greatest common depth of each station pair, and in substantial areas of the bottom parts of the sections no calculations can be made.) In the bottom water beneath our reference depth, stability layer number 6, the highest calculated velocities are along the western margin and have maxima between 2 and 3 cm s^{-1}. These values agree roughly with those calculated for this region by Wüst (1957) and Lynn (1971). Away from the western boundary the abyssal flow is weaker. In Fig. 11 the patterns are sinuous and lead to the alternation in sense of flow seen on the vertical sections.

Above the deep reference depth, the two sections show similar patterns. In the upper 1000 m along the continental slope the southward-flowing Brazil Current has maximum velocities of 30 to 40 cm s^{-1}. Along the slope between 2000 and 3500 m, a core of deep water moving southward is shown. In both sections, alternating bands of north and south velocities appear in the offshore regions. The subsurface core of northward flow anticipated by the choice of stability layer number 3 as a reference depth is found in both sections. We note that Wüst (1957) and Stommel (1958b) using *Meteor* and IGY data, respectively, also found such a subsurface core of northward-moving water.

7. Distributions on isopycnal surfaces

In Section 3 we have attempted to show that some of the recognized water masses are separated vertically

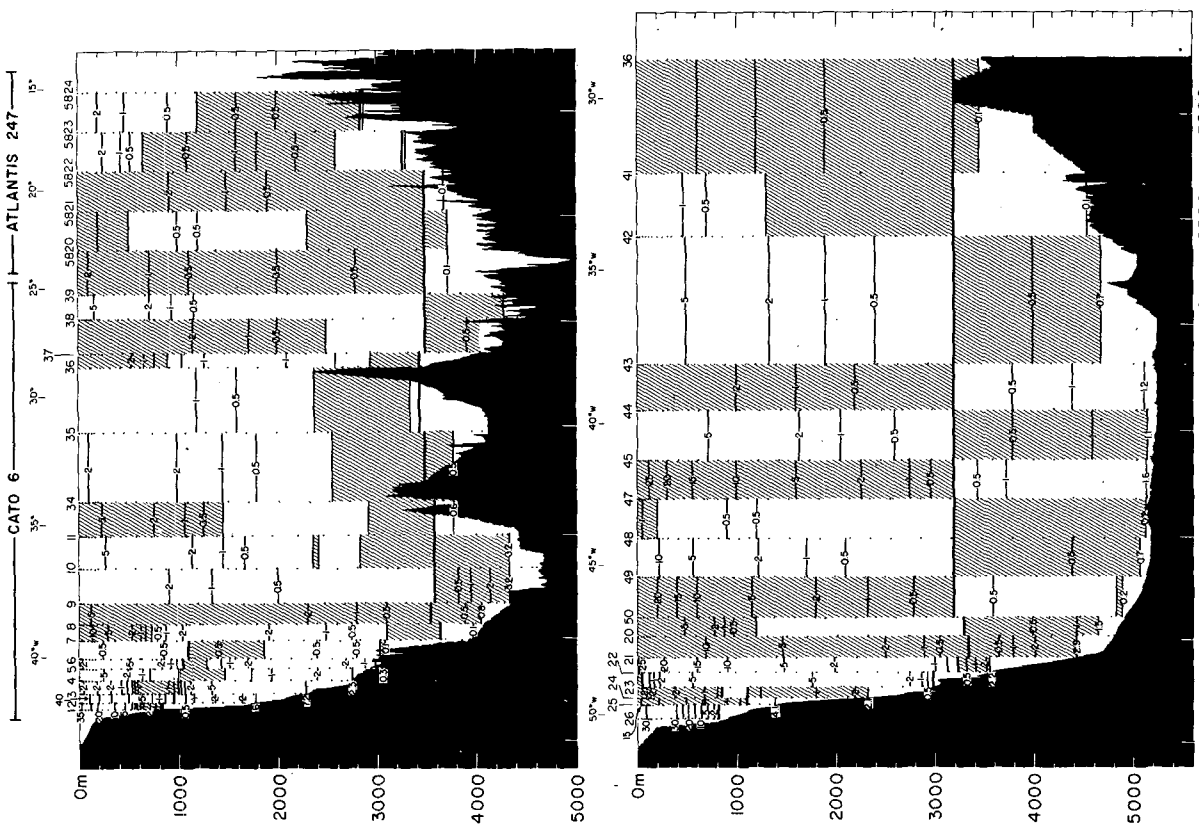

FIG. 13. Geostrophic speed (cm s^{-1}) on the two east-west lines calculated relative to the depths indicated by the heavy black line as discussed in the text. Hatched areas indicate northward flow, open areas southward.

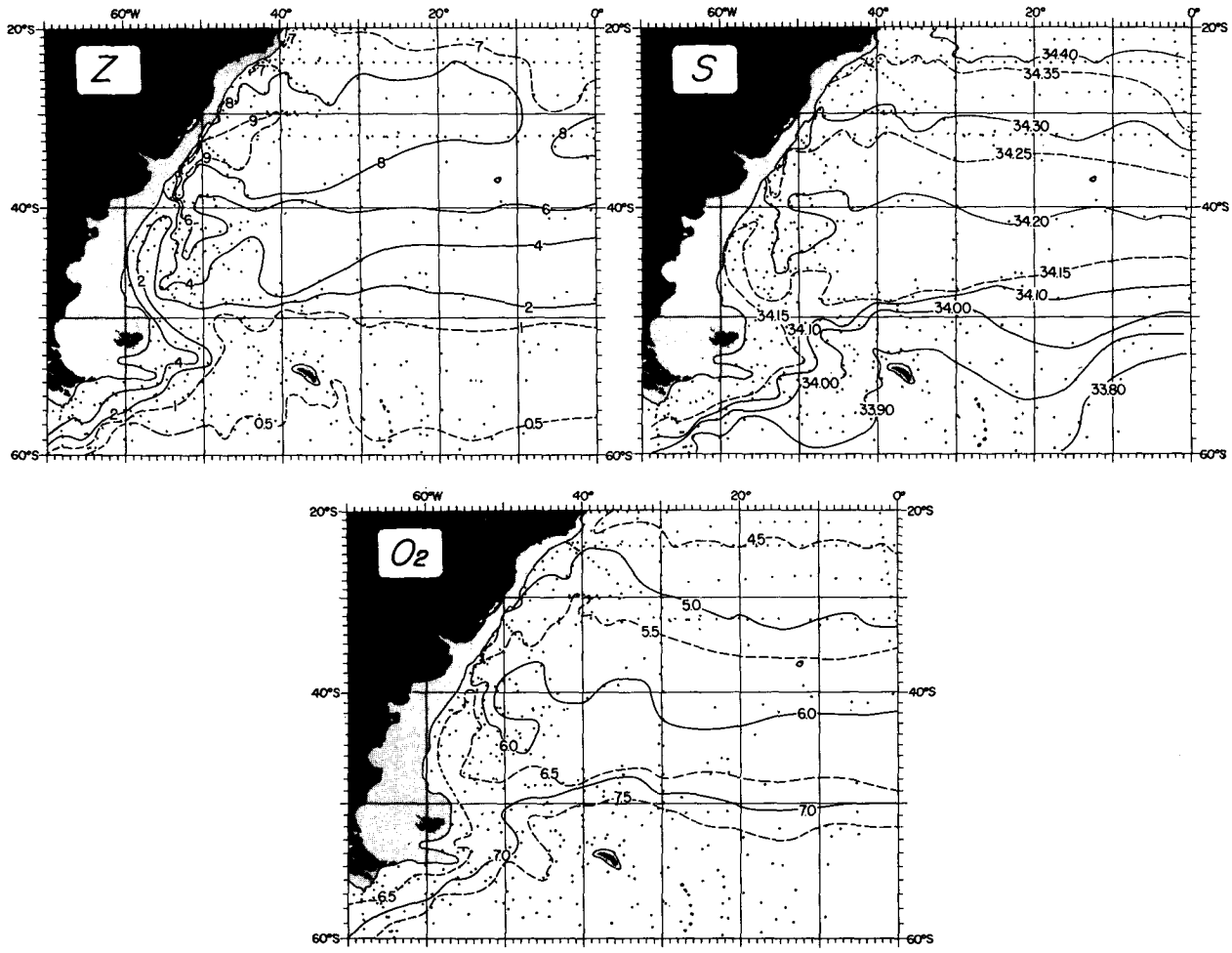

FIG. 14. Depth (hm), salinity (‰) and oxygen (ml l^{-1}) on the surface where $\sigma_0=27.18$.

by stability maxima. In this section we examine the characteristics of various layers by mapping them on isopycnal surfaces that lie between the maximum-stability strata. Seven isopycnal surfaces have been chosen to illustrate the characteristics and the circulation of the layers described in the preceding sections.

The layers represented are where:

1) $\sigma_0=27.18$, representing the Intermediate Water (Fig. 14);
2) $\sigma_0=27.535$, representing the upper branch of the Circumpolar Water (Fig. 15);
3) $\sigma_0=27.68$ (or $\sigma_2=36.90$), representing the core of the Circumpolar Water in the south and the upper part of the North Atlantic Deep Water in the north (Fig. 16);
4) $\sigma_0=27.76$ (or $\sigma_2=37.00$), representing Upper NADW (Fig. 17);
5) $\sigma_0=27.82$ (or $\sigma_2=37.09$), representing Lower NADW (Fig. 18);
6) $\sigma_0=27.845$ (or $\sigma_2=37.145$ or $\sigma_4=46.00$), representing the lower branch of the Circumpolar Water (Fig. 19);
7) $\sigma_2=37.23$ (or $\sigma_4=46.13$), representing Weddell Sea Deep Water (Fig. 20) and, unlike the others, lying within a stability stratum (number 8).

Nearly all of the isopycnals chosen are separated from the others by stability maxima over at least part of the area. Stability strata 4, 5, and 6 do not extend past about 45°S, where the NADW turns eastward, and we have chosen two isopycnals for the layer between stability strata 4 and 5. We do not illustrate Wüst's (1935) Middle NADW. The patterns of the characteristics are much like the other NADW, and in these latitudes the differences in characteristics are not clear.

a. Antarctic Intermediate Water

The shallowest isopycnal, with density parameter 27.18 in σ_0, lies between stability strata 2 and 3 and is taken to represent the layer called Subantarctic Intermediate Water by Wüst (1935). The depth of this isopycnal (Fig. 14) lies within a few meters' depth

of both the salinity minimum and oxygen maximum associated with this water. These extrema intersect the sea surface near 50°S, which is about the latitude of the outcrop of this isopycnal in southern winter (Böhnecke, 1936). Its depth is influenced by the Antarctic Circumpolar Current, where it lies shallowest, and by the subtropical anticyclonic gyre, in which it lies deepest, reflecting the general quasi-geostrophic circulation. The influence of both the Falkland Current and the Brazil Current is clear at this depth.

Wüst (1935) first described the Intermediate Water as originating from the high-oxygen and low-salinity, near-surface waters of the Antarctic and extending northward along the coast of South America, where it remained recognizable as a salinity minimum as far as 25°N. Later investigators, including Buscaglia (1971) who reviewed the earlier material, disagreed with the details of the trajectories proposed by Wüst (1935). Our results are in agreement with those of Buscaglia (1971), who argued that the northward flow along the west coast of South America extends only to about 40°S, with the Falkland Current, and that from there the water in this layer turns eastward in the subtropical anticyclonic gyre and flows around the eastern part of the gyre, reaching the coast of South America again north of 30°S. Its path may be represented roughly by the depth of the isopycnal (Fig. 14) or by the flow at 1000 db relative to 2000 db (Fig. 9). Between 30° and 40°S it is moving southward as part of the gyre and carrying waters of substantially higher salinity and lower oxygen than those in the Falkland Current (Fig. 14). Both the salinity minimum and the oxygen maximum extend throughout the gyre. These characteristics so dominate this density range that the salinity minimum can be seen as far north as 25°N (where it meets a higher salinity of similar density from the Mediterranean). The oxygen maximum, however, disappears within the intertropical shallow oxygen minimum and cannot be detected north of the equator (Wüst, 1935; Duedall and Coote, 1972).

b. The upper branch of the Circumpolar Water

The second isopycnal (27.535 in σ_0), lying between stability strata 3 and 4 in the north, was chosen to represent the northward extension of the upper part

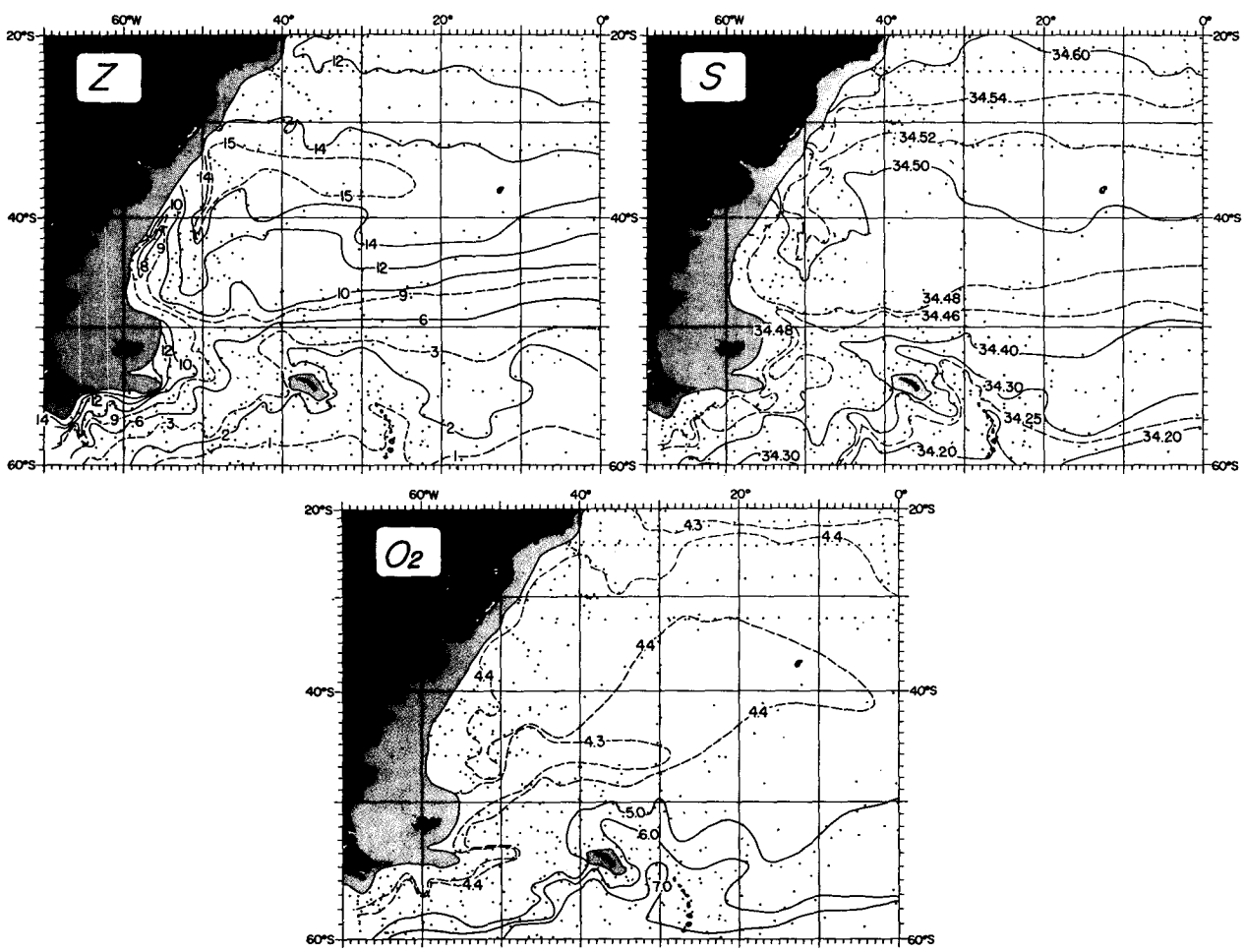

FIG. 15. As in Fig. 14 except $\sigma_0=27.535$.

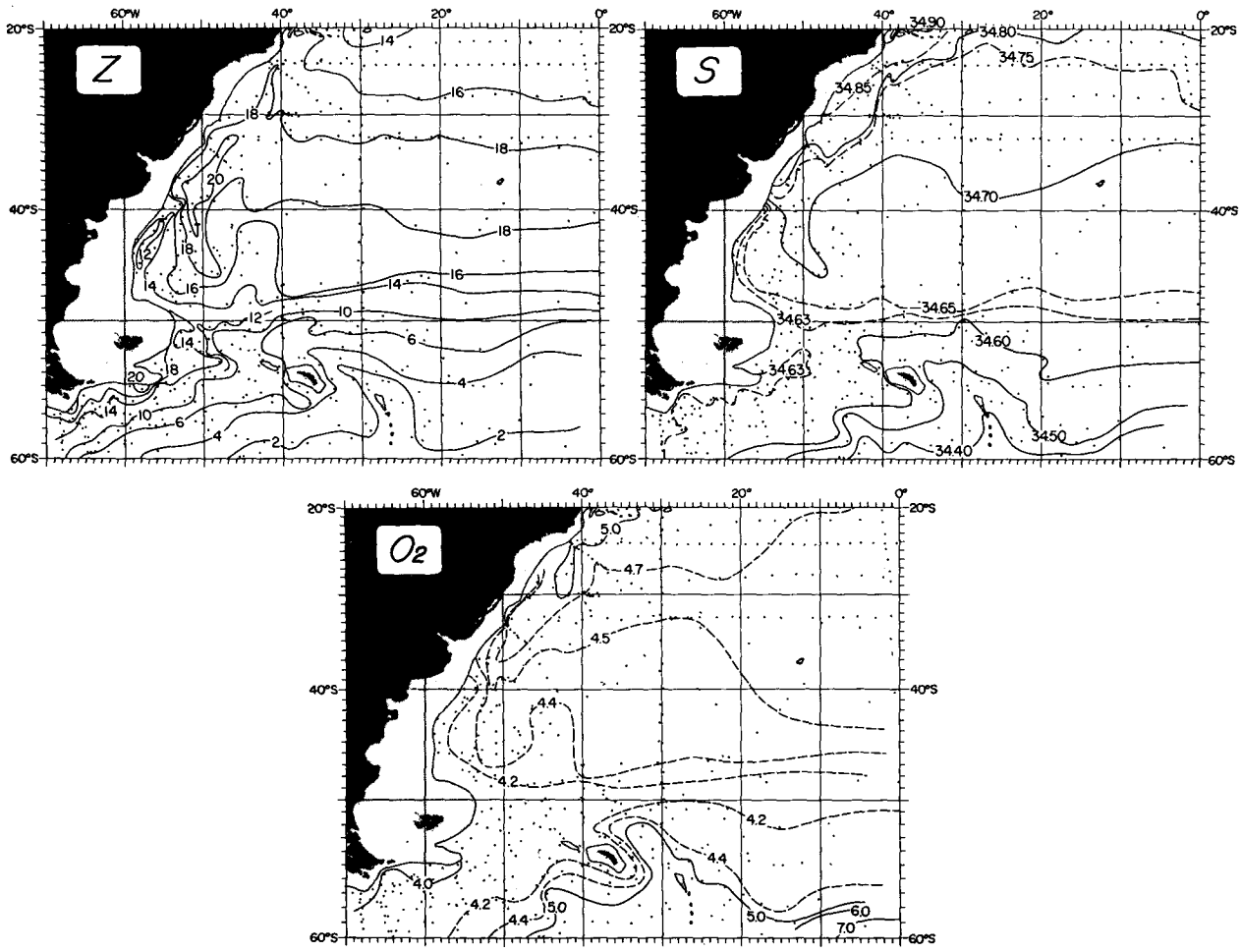

FIG. 16. As in Fig. 14 except $\sigma_0 = 27.68$ or $\sigma_2 = 36.90$.

of the Circumpolar Water. It lies within the pycnocline in the far south and at depths more than 1500 m within the anticyclonic gyre (Fig. 15). The Falkland Current flowing northward to about 40°S and the offshore return flow seen on Fig. 9 are clearly represented in the depth of the isopycnal. The depth maps (Figs. 14 and 15) indicate that the anticyclonic gyre is centered farther south here.

The principal characteristic of the upper branch of the Circumpolar Water is its low oxygen (Fig. 6a), originating from the waters west of the Drake Passage, but it also contains a temperature minimum south of 50°S, where it lies within the upper surface-cooled layer, and also at the northern end of the meridional section, where it lies just above the warm North Atlantic Deep Water (Fig. 6a).

The pattern of salinity on this isopycnal (Fig. 15) is much like that of the overlying Intermediate Water, though the values are higher. Both isopycnals lie near the sea surface in high latitudes and show the effect of the cold, low-salinity, high-oxygen surface waters. But where they lie deeper, in the northern part of the Drake Passage and in the western part of the Falkland Current, they also show the warmer, more saline and lower-oxygen characteristics of the deeper Circumpolar Water.

The lower oxygen of the deeper Circumpolar Water can be seen (Fig. 15) to extend from the Drake Passage northward with the Falkland Current and then eastward offshore as a tongue of low oxygen. It is surrounded on this isopycnal by a tongue of higher oxygen extending from the Antarctic around the anticyclonic gyre (Figs. 9 and 10).

In the north the oxygen decreases again by exchange with the waters of the thick oxygen-poor layer beneath the pycnocline in the subequatorial zone. Both Wüst (1935) and Wattenberg (1939) and, more recently, Duedall and Coote (1972) illustrated this low-oxygen layer. Its oxygen minimum lies much shallower than this isopycnal at the equator. The oxygen maximum of the Intermediate Water penetrates it almost to the equator in the western Atlantic. But on this isopycnal the oxygen decreases monotonically northward from the high value near 30° to 40°S to the minimum values near the equator; the lower oxygen to the north is not

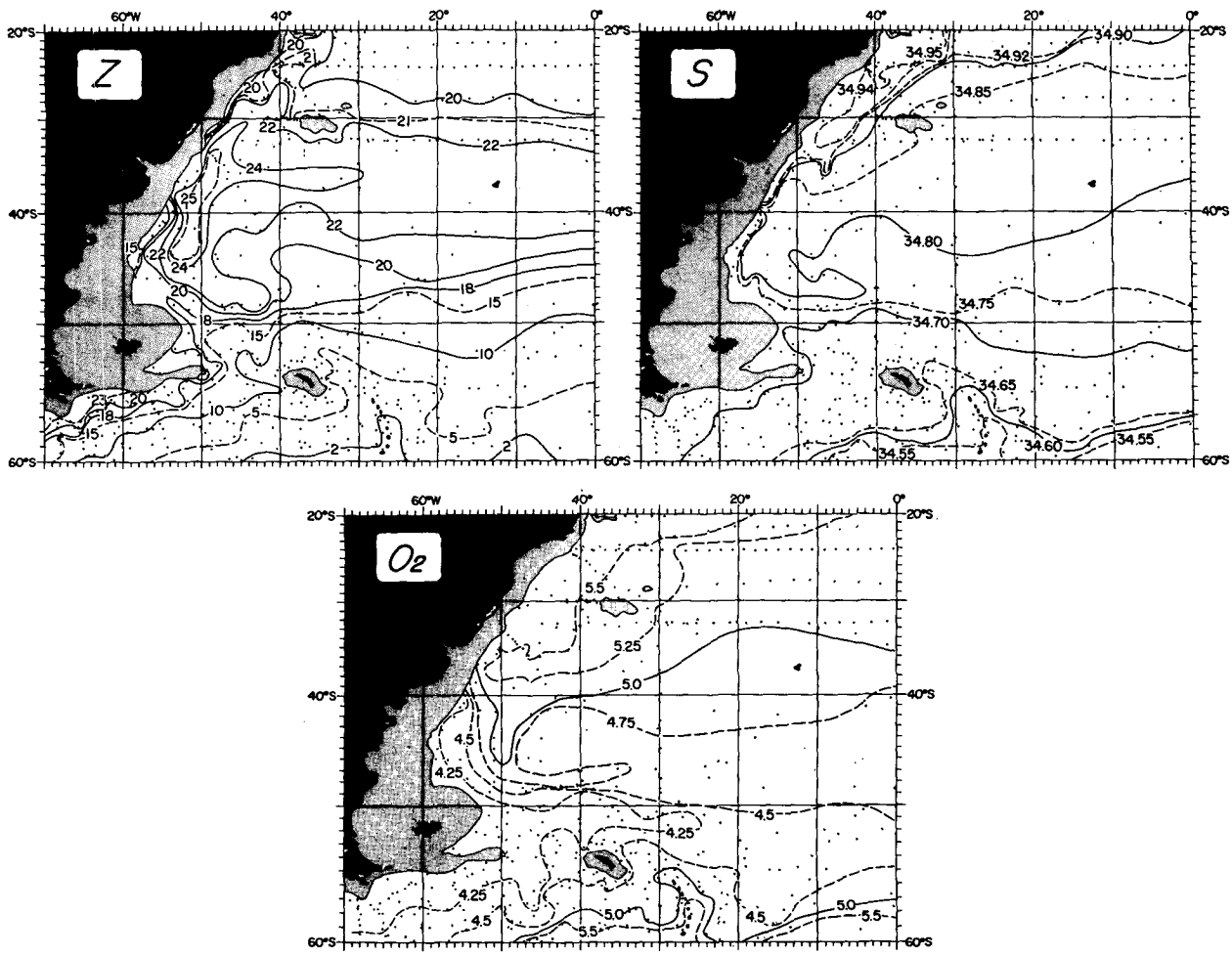

FIG. 17. As in Fig. 14 except $\sigma_0=27.76$ or $\sigma_2=37.00$.

from the Circumpolar Water but from the subequatorial zone.

c. Circumpolar Water and North Atlantic Deep Water

The third isopycnal (27.68 in σ_0, 36.90 in σ_2; Fig. 16), between stability strata 4 and 5 in the north, was chosen to illustrate the low-oxygen core of the Circumpolar Water where it crosses the meridional section (Fig. 6b). Toward the north, water of this density shows the dominance of the deep North Atlantic characteristics of high temperature, salinity and oxygen. This is most obvious at the northern end of the meridional section (Fig. 6a), where this isopycnal passes through the subsurface temperature maximum of the NADW, and the temperature rises abruptly. The salinity and oxygen maxima (Figs. 6a, b) lie slightly deeper. In the far south the isopycnal lies shallow, and exchange with the surface layer leads to lower temperature and salinity and higher oxygen. The layer of lowest oxygen (less than 4.2 ml l^{-1}) lies between about 45° and 55°S on the vertical section.

The shear field shown by the maps of relative geopotential anomaly (Figs. 9 and 10) is reflected by the depth of the isopycnal. The deeper Circumpolar Water entering from the Drake Passage is markedly higher in salinity and lower in oxygen (Fig. 16) than on the shallower isopycnals.

From the Drake Passage a band of low oxygen extends along this isopycnal eastward across the Atlantic, centered along about 50°S. Callahan (1972) has shown this feature and concluded that the low-oxygen values of the Circumpolar Water do not originate from the Atlantic subequatorial oxygen minimum, but from the Indian and Pacific oceans. This map and the meridional section are consistent with his conclusions.

It is now clear why stability strata 4, 5 and 6 do not extend farther south: they are associated with the NADW, which turns eastward north of about 50°S, and this density range is occupied south of there by the Circumpolar Water alone.

d. Upper North Atlantic Deeper Water

The salinity maximum that Wüst (1935) identified as the Upper North Atlantic Deep Water is seen on the

northern end of the meridional section at a σ_2 value of 37.00. This isopycnal rises southward to a σ_0 value of 27.76. It lies between the fourth and fifth stability strata where they exist in the north. The depth of this isopycnal (Fig. 17) reveals the western boundary shear, anticyclonic shear, and the Antarctic Circumpolar Current.

The extreme characteristics of the NADW are seen in the western boundary current as far south as about 40°S. Beyond there these waters still move southward, but farther offshore, and then turn eastward (Fig. 10). The influence of the Circumpolar characteristics is seen inshore to 40°S. Further south (near 60°S) the isopycnal lies near the sea surface (less than 200 m), and the effect of vertical exchange with the cold, fresher oxygen-rich surface waters is seen.

As in the case of the overlying layer ($\sigma_0=27.68$), this isopycnal shows the characteristics of the NADW in the north, the Circumpolar Water near 50°S, and the Antarctic waters in the far south. The salinity and oxygen patterns, as well as the shear (Figs. 17 and 10), show the high-salinity and high-oxygen waters turning eastward north of 50°S.

e. The Lower North Atlantic Deep Water

The isopycnal chosen to illustrate the Lower North Atlantic Deep Water is 27.82 in σ_0 (or 37.09 in σ_2 and 45.88 in σ_4) (Fig. 18). It lies between the fifth and sixth stability strata where they exist in the north. It corresponds in the northern end of the meridional section to the deeper oxygen maximum that Wüst (1935) used to identify his layer. Wüst (1935, 1943) had first assumed the origin of the Lower NADW to be from overturn within the Irminger Sea, but later Cooper (1955) recognized it as originating by overflow from the Norwegian-Greenland Sea extending to abyssal depths within the northern North Atlantic.

In an earlier study (Lynn and Reid, 1968) it was shown that in the North Atlantic the extreme characteristics flowing through the Denmark Strait from the Norwegian-Greenland Sea result in a maximum in potential density (σ_0) near 4000 m depth, near 45.92 or 45.93 in σ_4, and this maximum was taken to represent the Lower NADW in that study. In the northern North Atlantic the potential-density maximum, the oxygen maximum, and the 45.92–45.93 density range

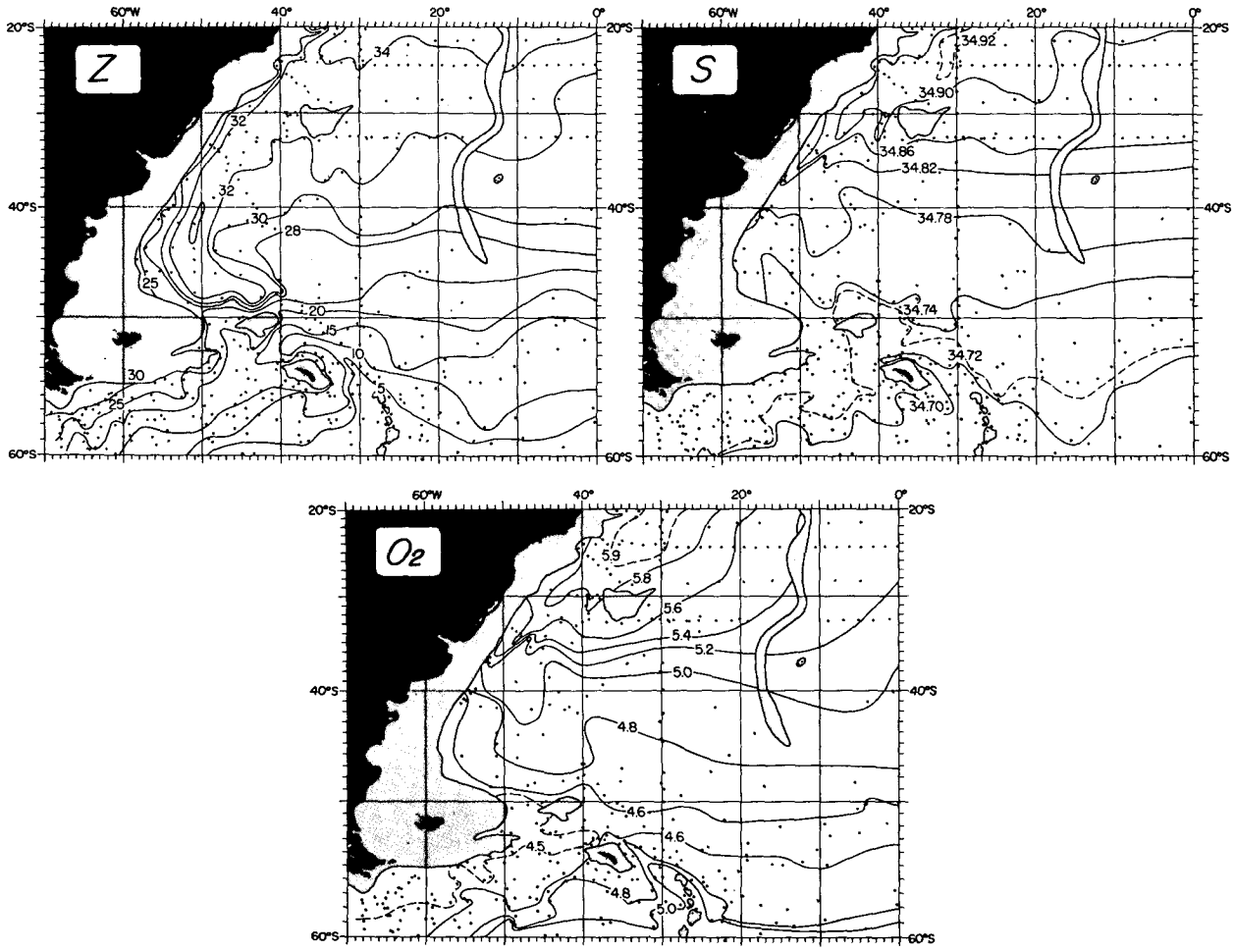

FIG. 18. As in Fig. 14 except $\sigma_0=27.82$ or $\sigma_2=37.09$.

are at about the same depth. Farther south, however, at the north end of our meridional section, the oxygen maximum overlies water from the Antarctic, with lower oxygen concentration, and is found at slightly shallower depths and lower densities. At our northern stations it lies at about 37.09 in σ_2 or 45.88 in σ_4. Still farther south the overlying minimum that separates it from Wüst's upper oxygen maximum (the Middle NADW) cannot be detected and only one deep oxygen maximum can be seen.

Deacon (1937) has mapped the salinity at the depth of the salinity maximum in the Circumpolar Water and indicated a cyclonic flow of more saline water into the southern Weddell Sea. This westward flow of higher salinity water along the southern boundary of the Weddell Sea was also indicated by Callahan (1972). Reid and Lynn (1971) mapped salinity distribution on the $\sigma_4=45.92$ surface, which lies within the North Atlantic Deep Water, and showed that the high salinity begins in the North Atlantic, extends southward and turns eastward with the Circumpolar Current.

The fifth and sixth stability strata, which encompass the LNADW as it moves southward from the North Atlantic, disappear from the meridional section as the LNADW turns eastward north of 45°S, and its density range south of there is made up of Circumpolar Water. Although stability strata 4 and 6, which enclose the whole body of North Atlantic Deep Water, are not detected south of 50°S, presumably they are to be found to the east, above and below the salinity maximum, for some undetermined distance downstream to the east. The salinity maximum of the NADW is itself seen, however, all the way into the Weddell Sea, with the lowest values at about 60°S. Since it originates in large part from the NADW, the Circumpolar Water itself is characterized by a salinity maximum and extends the high-salinity layer into the Indian and Pacific oceans (Deacon, 1937; Wüst, 1951; Stommel and Arons, 1960b; Reid and Lynn, 1971). The return flow from the Pacific through the Drake Passage still contains the maximum, which joins the original maximum extending southward from the North Atlantic where it meets the Circumpolar Current and turns eastward.

Within the Drake Passage the salinity maximum lies near 27.83 in σ_0, and at about the same value near 57°S on the meridional section. The southern part of the major high-salinity tongue extending from the North Atlantic is made up of water from the Drake Passage, as the oxygen distribution (Fig. 6b) also indicates. The separate salinity maximum, within the Weddell Sea, is at a higher density (above 27.84 in σ_0). It has reached the Weddell Sea by a flow from the Circumpolar Current around the cyclonic Weddell Sea gyre (Deacon, 1937; Gordon, 1971b; Reid and Lynn, 1971; Callahan, 1972), and in its shallow path south of the Circumpolar Current (Fig. 8) its upper salinity values have been reduced and the maximum lies at a higher density.

North of 40°S the depth of this isopycnal varies only from about 3200 to 3400 m, except along the western boundary, where it rises above 3000 m. Therefore, it lies only slightly above the waters whose characteristics indicate they have come from the south and are flowing northward along the western boundary. We assume a reversal in flow somewhere below this isopycnal and perhaps weak flow at its depths. In the higher latitudes the isopycnal slopes more steeply and the shear is better defined.

The salinity and oxygen fields show the southward extension of NADW as before, but along the western boundary the lower values from the Circumpolar Water extend farther north than in the overlying water. South of 45°S the Circumpolar Water appears to dominate the NADW.

f. The lower branch of the Circumpolar Water

The isopycnal chosen to represent the oxygen minimum of the Lower Circumpolar Water that lies beneath the NADW in the Cato area is 46.00 in σ_4, which extends southward and upward as 37.145 in σ_2 and 27.845 in σ_0 (Fig. 19). It lies within the oxygen minimum between the sixth and seventh stability strata, where the LNADW lies above this minimum. South of there it lies below the principal oxygen minimum of the Circumpolar Water (between 45° and 55°S; Fig. 6a) and in the Weddell Sea it lies so near the surface that the oxygen minimum is below it.

The oxygen minimum we have used to define the Lower Circumpolar Water disappears just north of the Rio Grande Rise. It is last seen at Cato stations 9 and 10 on the northern section (Fig. 3a). North of there the oxygen concentration rises to more than 5.5 ml l^{-1} (Fig. 19), much higher than the underlying waters farther south. The increase must be from the overlying LNADW of high oxygen content. The salinity increases also.

South of the Rio Grande Rise, however, the characteristics on the isopycnal suggest a dominant Circumpolar origin. The isopycnal slopes upward to the west along the western boundary north of 50°S. We assume from the characteristics that the flow is northward along the western boundary, and therefore from the density field we infer that the northward flow there is increasing toward the bottom. The gyre defined by the deep trough in the depth of the isopycnal, which indicates an anticyclonic gyre relative to the deeper water, must be interpreted instead as a cyclonic gyre relative to the overlying water. This sort of flow is illustrated by the shear at 4000 db relative to 3500 db (Fig. 11).

The dense bottom waters of the central North Atlantic are less saline than any North Atlantic source can provide at these densities. The source of this less

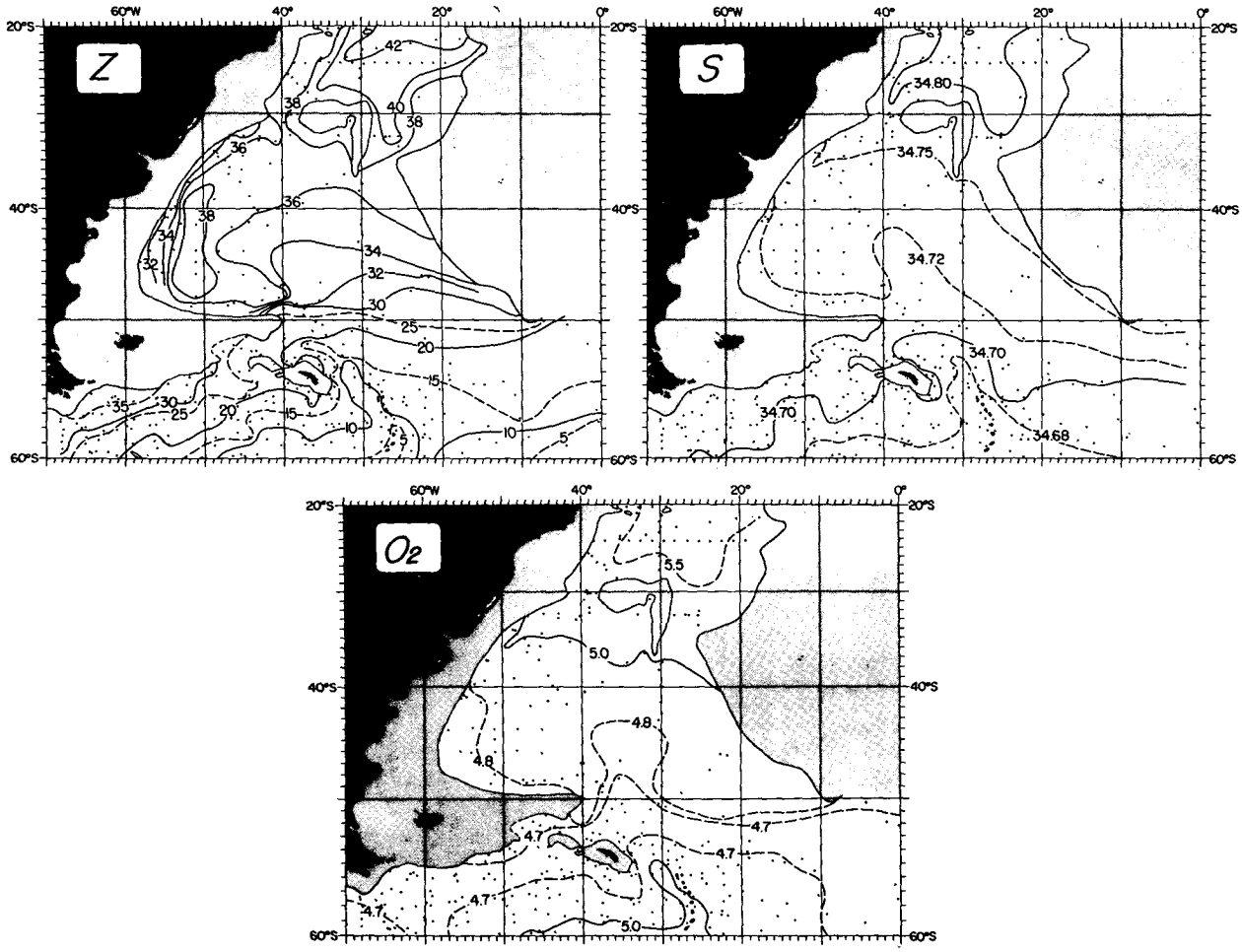

FIG. 19. As in Fig. 14 except $\sigma_0=27.845$ or $\sigma_2=37.145$ or $\sigma_4=46.00$.

saline bottom water must be the northward flow near and below this isopycnal (46.00 in σ_4). In the latitudes considered here, the northward flow appears to take place along the western boundary.

The cyclonic gyre would carry the more saline, oxygen-rich waters southward along its eastern rim, joining the Circumpolar Current near 45°S. The salinity and oxygen patterns on the isopycnal (Fig. 19) are consistent with such flow.

g. The Weddell Sea Deep Water

Within the Weddell Sea this layer lies between the seventh and ninth stability strata. The characteristics within it change monotonically downward from the temperature, salinity, and nutrient maxima and oxygen minimum of the overlying Circumpolar Water to the underlying newly formed bottom water, which is colder, less saline, richer in oxygen, and poorer in nutrients. Its characteristics are intermediate in value between those of these adjacent layers and might be accounted for by vertical diffusion between those two layers within the Weddell Sea cyclonic gyre. Its minimum density (in stability stratum 7) is greater than that of any of the water entering from the Pacific, and it must therefore originate east of the Drake Passage, within the Weddell Sea gyre.

Because there is such a large body of water beneath the seventh stratum, and the layer we call Weddell Sea Deep Water is so thick, we might have chosen a wide range of isopycnals to represent the water. The vertical changes in characteristics, however, are monotonic below the seventh stratum, and the patterns would be about the same for any isopycnal chosen. We choose the isopycnal that represents the densest waters that extend throughout the meridional section as far as the Rio Grande Rise (46.13 in σ_4, extending southward and upward as 37.23 in σ_2; Fig. 20). This isopycnal intersects the bottom just beyond the Rio Grande Rise near 25°S.

The depth of this isopycnal is given in Fig. 20. It lies very near the bottom over most of the section and at mid-depth within the Weddell Sea. Although it extends down to 5000 m, the depth of this isopycnal has about the same shape as those above it; the flow around the Argentine Basin must be in the opposite

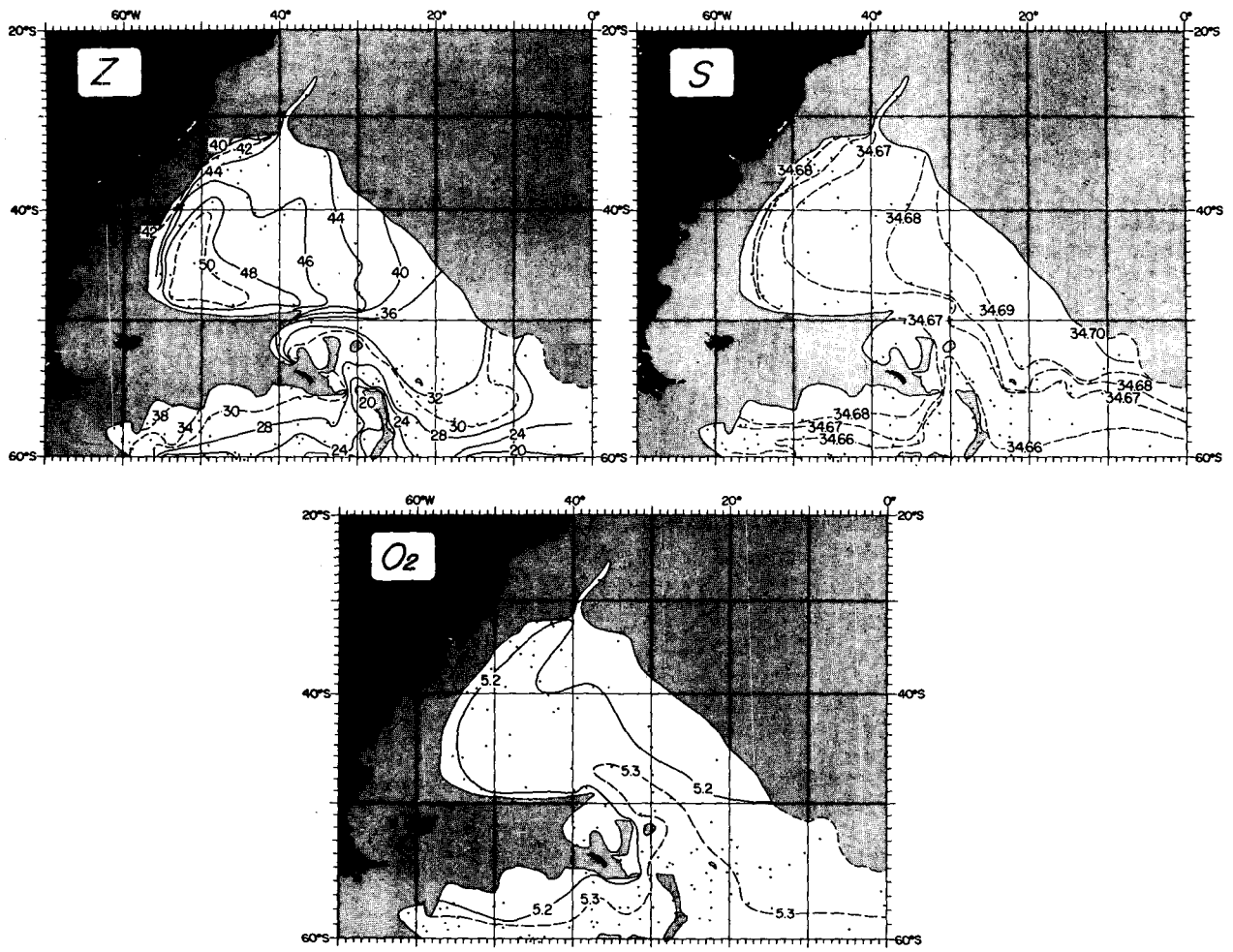

FIG. 20. As in Fig. 14 except $\sigma_2=37.23$ or $\sigma_4=46.13$.

sense, however, as a cyclonic gyre. Within the Argentine Basin the shear at 4000 db relative to 3500 db (Fig. 11) may be taken to illustrate its flow. The low salinity values and high oxygen (Fig. 20) extending equatorward along the western boundary can best be accounted for by such a flow, and the higher salinities and lower oxygens on the eastern side of the Argentine Basin are consonant with a return flow after some vertical exchange with the overlying Circumpolar Water, which is higher in salinity and lower in oxygen.

The isopycnal defined by $\sigma_4=46.13$ is also the approximate density of the eighth stability stratum. We have no explanation for this stratum, which appears within the Weddell Sea Deep Water. It is not so clearly defined by the available data as we should like, but is not so marginal as to be discounted entirely. It does not appear to separate layers of different characteristics in temperature, salinity, or oxygen.

h. Weddell Sea Bottom Water

At the southern end of the meridional section lies a layer in which the density increases suddenly to more than 46.25 in σ_4. Temperature and nutrients decrease markedly and oxygen increases.

Carmack and Foster (1977) have shown a distinct layer of bottom water within the Weddell Sea with potential temperature below -0.7°C and defined this as Weddell Sea Bottom Water.

The section reveals a stability stratum (numbered 9) that overlies this layer at the southern station; on the other four stations the stability stratum is too thin to reveal clearly whether the stability maximum lies above or within the layer. At other stations in the vicinity the stability maximum is more clearly above the bottom layer.

We do not illustrate the characteristics of this water on an isopycnal surface, but note that Carmack and Foster (1975) have mapped the potential temperature between 60° and 20°W on an isopycnal ($\sigma_4=46.22$ below 3000 db) and indicate an eastward flow just south of 60°S. We do not find this WSBW or stability stratum 9 north of 60°S, except where there is some indication of it in the South Sandwich Trench up to 55°S.

8. Summary

We have examined the characteristics of the waters of the southwestern Atlantic Ocean using the three concepts of geostrophic flow, isopycnal flow and mixing, and the separation of layers by intervening high-stability strata.

Combining information from the vertical shear (taken from the density field) with inferences about the sense of flow at various levels (taken from the distribution of characteristics both in the vertical sections and along isopycnals), we find a subtropical anticyclonic gyre, not only in the near-surface layer, but also extending to depths of about 3000–3500 m.

The center of the anticyclonic gyre is compressed tightly against the western boundary. The strongest flow is the poleward western boundary current, but a substantial part of the equatorial flow of the gyre is found just offshore from the poleward flow.

An equatorward western boundary current (the Falkland Current) extends from the Antarctic Circumpolar Current in the Drake Passage to about 40°S, where it meets the poleward boundary current of the anticyclonic gyre, and the two currents turn offshore toward the east as part of the Antarctic Circumpolar Current.

At greater depths the denser waters from the Weddell Sea flow equatorward also, as a western boundary current around the Scotia Arc and through the Argentine Basin. Unlike the overlying waters, these abyssal waters continue northward past 40°S beneath the anticyclonic gyre and extend along the western boundary to the Rio Grande Rise, where some part of the flow turns cyclonically around the Basin and back toward the Antarctic Circumpolar Current.

The waters that fill the southwestern Atlantic Ocean enter from the North Atlantic Ocean, from the Pacific Ocean through the Drake Passage, and from the Weddell Sea. They have acquired their characteristics in these different areas and lie at depths corresponding to their densities; these depths then must vary horizontally according to the geostrophic structure of the density field.

They circulate within the system described above, and although both lateral and vertical mixing take place, their initial characteristics are sufficiently preserved to be identified over long distances. They are of different density ranges, and, where two vertically adjacent layers are of substantially different densities, there may be a sharper density gradient, or stability maximum, between them. In spite of the vertical exchange processes, these stability features are extended and maintained over long distances by the continuing lateral circulation and lateral mixing.

The waters entering from the Pacific through the Drake Passage are less dense than those formed in the Weddell Sea, and, when they override the Weddell Sea waters, the difference in density leads to the formation of such a maximum in stability. Both the Circumpolar Water and the denser water from the Weddell Sea extend into the Argentine Basin, and the stability maximum between them is detectable as far as the Rio Grande Rise.

The Circumpolar Water extends into the South Atlantic as an oxygen-poor, nutrient-rich layer with a density range encompassing that of the oxygen-rich and nutrient-poor waters from the North Atlantic. Where the NADW extends into the South Atlantic it separates the layer of Circumpolar Water into two layers above and below, separated from the NADW by high-stability strata. The NADW turns eastward with the West Wind Drift, and these two stability maxima are observed only north of 50°S, in the area where the oxygen minimum and nutrient maximum are split by the NADW.

The Intermediate Water originates from the surface and near-surface waters of high latitudes and flows into the South Atlantic above the Circumpolar Water and below the upper pycnocline; the density differences are great enough to be marked by a stability maximum both above and below the Intermediate Water.

In particular, we have shown that the Circumpolar Water encompasses the density range of the NADW, from which its high salinity derives, and that within the South Atlantic the two great oxygen minima, above and below the NADW, have come from the Antarctic Circumpolar Current.

We have shown that the Circumpolar Water also contributes to, and perhaps provides, the shallow layer of high nutrients within the Weddell Sea and the deep layer of high nutrients within the central South Atlantic Ocean.

The designation "Antarctic Bottom Water" can lead to some confusion. The densest Antarctic Water is formed within the Weddell Sea and extends eastward from there as an abyssal layer that is low in temperature, salinity, and nutrients and high in oxygen. It does not extend into the Argentine Basin. Instead it is the Weddell Sea Deep Water, with characteristics intermediate between those of the overlying Circumpolar and underlying bottom water in the Weddell Sea, that extends northward into the Argentine Basin as a western boundary current and, with the lower branch of the Circumpolar Water, carries the characteristics of Antarctic waters into the abyssal Atlantic Ocean.

Acknowledgments. This paper represents one of the results of research supported by the Office of Naval Research, the National Science Foundation, and the Marine Life Research Program, the Scripps Institution's component of the California Cooperative Fisheries Investigations, a project sponsored by the Marine Research Committee of the State of California. We are grateful for discussions with many other investigators during the several years of preparation of this

manuscript, and we express especially our thanks to Bruce Warren and Eddy Carmack for reading and commenting upon the manuscript.

REFERENCES

Boguslavskii, S. G., and L. A. Koveshnikov, 1965: Subantarctic intermediate current in the Atlantic. *Izv. Akad. Nauk SSSR, Fiz. Atmos. Okeana*, **1**, 233–235. [English translation: *Atmos. Oceanic Phys.*, **1**, 138–139.]

Böhnecke, G., 1936: Die Temperatur. *Wiss. Ergebn. dtsch. Atlant. Exped. "Meteor"*, **5**(2), 187–249.

Burckle, L. H., and D. Stanton, 1975: Distribution of displaced antarctic diatoms in the Argentine Basin. Proc. Third Symp. Recent and Fossil Marine Diatoms, Kiel, Sept. 9–13, 1974, R. Simonsen, Ed., *Nova Hedwigia*, Beiheft 53, 283–292.

Buscaglia, J. L., 1971: On the circulation of the Intermediate Water in the southwestern Atlantic Ocean. *J. Mar. Res.*, **29**, 245–255.

Callahan, J. E., 1972: The structure and circulation of deep water in the Antarctic. *Deep-Sea Res.*, **19**, 563–575.

Carmack, E. C., 1973: Silicate and potential temperature in the deep and bottom waters of the western Weddell Sea. *Deep-Sea Res.*, **20**, 927–932.

——, and T. D. Foster, 1975: On the flow of water out of the Weddell Sea. *Deep-Sea Res.*, **22**, 711–724.

——, and ——, 1976: Water masses and circulation in the Weddell Sea. *Proc. SCOR/SCAR Polar Oceans Conf.*, Montreal, May 1974 (in press).

Clowes, A. J., 1933: Influence of the Pacific on the circulation in the southwest Atlantic Ocean. *Nature*, **131**, 189–191.

Cooper, L. H. N., 1955: Deep water movements in the North Atlantic as a link between climatic changes around Iceland and biological productivity of the English Channel and Celtic Sea. *J. Mar. Res.*, **14**, 347–362.

Craig, H., Y. Chung and M. Fiadeiro, 1972: A benthic front in the South Pacific *Earth Planet. Sci. Lett.*, **16**, 50–65.

Deacon, G. E. R., 1937: The hydrology of the southern ocean. *Discovery Rep.*, **15**, 1–124.

Defant, A., 1941: Quantitative Untersuchungen zur Statik und Dynamik des Atlantischen Ozeans. *Wiss. Ergebn. dtsch. atlant. Exped. "Meteor,"* **6**(2) (5), 191–260.

Duedall, I. W., and A. R. Coote, 1972: Oxygen distribution in the South Atlantic. *J. Geophys. Res.*, **77**, 496–498.

Edmond, J. M., and G. C. Anderson, 1971: On the structure of the North Atlantic Deep Water. *Deep-Sea Res.*, **18**, 127–133.

Ewing, M., S. L. Eittreim, J. I. Ewing and X. Le Pichon, 1971: Sediment transport and distribution in the Argentine Basin. 3. Nepheloid layer and processes of sedimentation. *Phys. Chem. Earth*, **8**, 49–77.

Fuglister, F. C., 1957: Oceanographic data from *Crawford* Cruise Ten obtained for the International Geophysical Year of 1957–58. Ref. No. 57–34, Woods Hole Oceanographic Institution, 129 pp.

——, 1963: Gulf Stream '60. *Prog. Oceanogr.*, **1**, 265–373.

Gordon, A. L., 1967: Structure of Antarctic waters between 20°W and 170°W. *Antarctic Map Folio Series*, V. C. Bushnell, Ed., Amer. Geogr. Soc., Folio 6, 10 pp,. 14 plates.

——, 1971a: Oceanography of Antarctic Waters. *Antarctic Oceanology I, Antarctic Research Series*, 15, J. L. Reid, Ed., Amer. Geophys. Un., 169–203.

——, 1971b: Recent physical oceanographic studies of antarctic waters. Research in the Antarctic, Symposium at A.A.A.S. Meeting, Dallas, Dec., 1968, L. O. Quam, Ed., A.A.A.S. Publ. No. 93, 609–629.

Hamon, B. V., 1970: Western boundary currents in the South Pacific *Scientific Exploration of the South Pacific*, W. S. Wooster, Ed., Nat. Acad. Sci., Washington, D. C., 50–59.

Hesselberg, T., and H. U. Sverdrup, 1914: Die Stabilitätsverhältnisse des Seewassers bei vertikalen Verschiebungen. *Bergens Mus. Arbok*, No. 15, 17 pp.

Iselin, C. O'D., 1936: A study of the circulation of the western North Atlantic. *Pap. Phys. Oceanogr. Meteor.*, **4**, 1–101.

Johnson, D. A., S. E. McDowell, J. L. Reid and W. C. Patzert, 1974: On the flow of Antarctic Bottom Water through the Vema Channel. Presented at Amer. Geol. Soc. Annual Meeting, Nov. 1974, Miami Beach, Fla., Abstracts with Programs, **6**, 811.

Lynn, R. J., 1971: On potential density in the deep South Atlantic Ocean. *J. Mar. Res.*, **29**, 171–177.

——, and J. L. Reid, 1968: Characteristics and circulation of deep and abyssal waters. *Deep-Sea Res.*, **15**, 577–598.

Menzel, D. W., and J. H. Ryther, 1968: Organic carbon and the oxygen minimum in the South Atlantic Ocean. *Deep-Sea Res.*, **15**, 327–337.

Metcalf, W. G., 1958: Oceanographic data from *Crawford* Cruise 16, 1 Oct.–11 Dec. 1957, for the International Geophysical Year of 1957–58. Ref. No. 58–31, Woods Hole Oceanographic Institution, 125 pp.

——, 1959: Oceanographic data from the Caribbean Sea—*Crawford* Cruise 17, February–March 1958, for the International Geophysical Year of 1957–58. Ref. No. 59–9, Woods Hole Oceanographic Institution, 90 pp.

Miller, A. R., 1960: Oceanographic data from *Atlantis* Cruise 247—January–June 1959 for the International Geophysical Year of 1957–58. Ref. No. 60–40, Woods Hole Oceanographic Institution, 144 pp.

Montgomery, R. B., and M. J. Pollak, 1942: Sigma-T surfaces in the Atlantic Ocean. *J. Mar. Res.*, **5**, 20–27.

Pingree, R. D., and G. K. Morrison, 1973: The relationship between stability and source waters for a section in the Northeast Atlantic. *J. Phys. Oceanogr.*, **3**, 280–285.

Reid, J. L., Jr., 1961: On the geostrophic flow at the surface of the Pacific Ocean with respect to the 1,000-decibar surface. *Tellus*, **13**, 489–502.

——, and R. J. Lynn, 1971: On the influence of the Norwegian-Greenland and Weddell seas upon the bottom waters of the Indian and Pacific oceans. *Deep-Sea Res.*, **18**, 1063–1088.

——, and W. D. Nowlin, Jr., 1971: Transport of water through the Drake Passage. *Deep-Sea Res.*, **18**, 51–64.

——, and P. F. Lonsdale, 1974: On the flow of water through the Samoan Passage. *J. Phys. Oceanogr.*, **4**, 58–73.

——, and R. S. Arthur, 1975: Interpretation of maps of geopotential anomaly for the deep Pacific Ocean. *J. Mar. Res.*, **33** (Suppl.), 37–52.

Schubert, O. von, 1935: Die Stabilitätsverhältnisse im Atlantischen Ozean. *Wiss. Ergebn. dtsch. atlant. Exped. "Meteor,"* **6**(2) (1), 54 pp.

Sessions, M., 1975: Improved free vehicle current meter system. *Exposure*, **3**, 1–4.

Stommel, H., 1958a: The abyssal circulation. *Deep-Sea Res.*, **5**, 80–82.

——, 1958b: *The Gulf Stream.* University of California Press and Cambridge University Press, 202 pp.

——, and A. B. Arons, 1960a: On the abyssal circulation of the world ocean—I. Stationary planetary flow patterns on a sphere. *Deep-Sea Res.*, **6**, 140–154.

——, and ——, 1960b: On the abyssal circulation of the world ocean—II. An idealized model of the circulation pattern and amplitude in oceanic basins. *Deep-Sea Res.*, **6**, 217–233.

Sverdrup, H. U., M. W. Johnson and R. H. Fleming, 1942: *The Oceans; their Physics, Chemistry,* and *General Biology.* Prentice Hall, 1087 pp.

Wattenberg, H., 1939: Atlas zu die Verteilung des Sauerstoffs im atlantischen Ozean. *Wiss. Ergebn. dtsch. atlant. Exped. "Meteor,"* **9** (Atlas), 72 plates.

Worthington, L. V., 1958: Oceanographic data from the R.R.S. *Discovery II*—International Geophysical Year Cruises One

and Two, 1957. Ref. No. 58–30, National Institute of Oceanography and Woods Hole Oceanographic Institution, 152 pp.

——, and W. G. Metcalf, 1961: The relationship between potential temperature and salinity in deep Atlantic water. *Rapp. P.-V. Réun., Cons. Int. Explor. Mer*, **149**, 122–128.

——, and W. R. Wright, 1970: North Atlantic Ocean atlas of potential temperature and salinity in the deep water including temperature, salinity and oxygen profiles from the *Erika Dan* cruise of 1962. Woods Hole Oceanographic Institution Atlas Series, 2, 24 pp., 58 plates.

Wright, W. R., 1970: Northward transport of Antarctic Bottom Water in the Western Atlantic Ocean. *Deep-Sea Res.*, **17**, 367–371.

Wüst, G., 1935: Die Stratosphäre. *Wiss. Ergebn. dtsch. Atlant. Exped. "Meteor,"* **6**(1), 109–288.

——, 1943: Der subarktische Bodenstrom in der westatlantischen Mulde. *Ann. Hydrogr. Marit. Meteorol.*, **71**, 249–255.

——, 1951: Über die Fernwirkungen antarktischer und nordatlantischer Wassermassen in den Tiefen des Weltmeeres. *Naturwiss. Rundsch.*, **3**, 97–108.

——, 1957: Stromgeschwindigkeiten und Strommengen in den Tiefen des Atlantischen Ozeans unter besonderer Berücksichtigung des Tiefen- und Bodenwassers. *Wiss. Ergebn. dtsch. atlant. Exped. "Meteor,"* **6**(2) (6), 260–420.

Wyrtki, K., 1975: Fluctuations of the dynamic topography in the Pacific Ocean. *J. Phys. Oceanogr.*, **5**, 450–459.